An ab Initio Study of Transition Structures and Associated Products in $[ZnOHCO_2]^+$, $[ZnHCO_3H_2O]^+$, and $[Zn(NH_3)_3HCO_3]^+$ Hypersurfaces. On the Role of Zinc in the Catalytic Mechanism of Carbonic Anhydrase

O. Jacob,[†,§] R. Cardenas,[§] and O. Tapia*[,‡]

Contribution from the Department of Molecular Biology, BMC-SLU, Box 590, S-75124 Uppsala, Sweden, and Department of Physical Chemistry, Uppsala University, Box 532, S-75121 Uppsala, Sweden. *Received January 2, 1990*

Abstract: The zinc hydroxide mechanism has been studied on a series of zinc complexes with and without ammonia coordination shell in the RHF SCF framework using extended basis sets, (14s,9p,5d) for Zn and (9s,5p) for O, C, and N. Saddle points, minima and related force constants, and geometries are reported for the energy hypersurfaces of $[ZnOHCO_2]^+$ and $[ZnHCO_3H_2O]^+$. In the $[ZnOHCO_2]^+$ hypersurface, transition structures corresponding to interconversion and productive binding of bicarbonate (monodentate complex with zinc) have been characterized. On the $[ZnHCO_3H_2O]^+$ hypersurface active and passive (displacement) solvation effects on HCO_3^- binding to zinc have been studied. The MP2 reactive energy profile basically conserves the inverted shape found at the SCF level. For the ammonia liganded complexes calculations, the following points have been examined: (i) zinc hydroxide nucleophilicity and basicity compared to the bare zinc results; (ii) effects on bicarbonate/water exchange energy balance; (iii) characterization of the monodentate HCO_3^- binding structure on the energy hypersurface spanned by the full set of geometrical variables, followed by an exploration of the resulting transition vector; and (iv) pyramidal and tetrahedral coordination models of zinc cation. The saddle point character of bicarbonate monodentate binding to zinc is conserved; if HCO_3^- is allowed to move along one of its transition vector directions (which describes an intramolecular rotation-like motion of the HCO_3^- moiety) a channel toward the interconversion process is opened. Along this reactive pathway, the coordination state of zinc oscillates between tetra- and pentacoordination. The coordination shell accentuates the inverted nature for the energy profile leading to interconversion. This profile can be naturally correlated to the molecular events of the zinc hydroxide mechanism. Bare zinc roles in the carbon dioxide hydroxylation can be summarized as the following: (i) inhibition of simple hydroxide nucleophilicity strength; (ii) carbon dioxide carbonyl activation; (iii) well-defined interconversion pathway at the bottom of an inverted energy profile with low activation barrier; and (iv) formation of a monodentate bicarbonate complex having a saddle point nature: a bicarbonate productive binding. Molecular docking of the ab initio stationary geometries onto the active site of the X-ray structures of various CAs have been performed by using FRODO software. A detailed molecular mechanism can be proposed where Thr-199 plays a central role.

I. Introduction

The zinc cation plays a central role in the catalytic mechanism of carbonic anhydrases (EC 4.2.1.1).[1,2] These enzymes catalyze the reversible hydration of carbon dioxide and dehydration of bicarbonate. The zinc hydroxide mechanism has been successfully used in organizing a wealth of experimental studies.[1-4] Its first stage consists of a zinc-bound water activation via a deprotonation process. In its second stage, the zinc-bound hydroxide performs a nucleophilic attack onto carbon dioxide forming a Zn-bound bicarbonate; this latter must be exchanged with one water molecule and released from the active site. When the reaction takes place in the opposite direction, bicarbonate must displace a zinc-bound water and binds to zinc. Microscopic reversibility requires the structure of the zinc-bound bicarbonate formed along the hydration and dehydration pathways to be the same (productive binding). Thus, the chemical processes involved in the second stage (interconversion), which is the subject of the present study, can be simply sketched as

$$[E\text{-}ZnOH]^+ + CO_2 \rightarrow [E\text{-}ZnOH{\cdot}CO_2]^+ \rightarrow [E\text{-}ZnHCO_3]^+ \xrightarrow{H_2O} [E\text{-}ZnH_2O]^{2+} + HCO_3^-$$

From the theoretical standpoint, the importance of the zinc cation in the enzyme reaction can be hinted when one looks at carbon dioxide hydroxylation in vacuo. This reaction corresponds to a nucleophilic attack of a negative ion onto a neutral molecule; from simple electrostatics the potential energy shape would correspond to an exothermic process. This is confirmed in the ab initio calculations reported by us and other authors; these results systematically show a strongly exothermic reaction (ca. 90 Kcal/mol) without formation of stable intermediates; consequently, no transition structure has been found along the reaction coordinate. Since the enzyme catalyzes the reversible interconversion reaction, one should expect the environments including of course zinc cation at the active site to dramatically change the thermal balance and the reaction profile between reactants and products for the zinc hydroxide mechanistic steps.

The molecular reorganization events taking place at the coordination sphere of zinc are relatively simple. A number of important theoretical works have been designed to characterize the role played by zinc there. Approximate as well as ab initio molecular orbital techniques,[5-10] albeit some of these[8] at a relatively low basis set level representation, have been used. Until now, however, there is not a fully satisfactory theoretical explanation in terms of energy hypersurfaces obtained at a high level of basis set and with a proper characterization of the stationary points

* Author to whom correspondence must be addressed.
† Permanent address: Merrell Dow Research Institute, 16 Rue d'Ankara, 67084 Strasbourg, France.
‡ Department of Physical Chemistry.
§ Department of Molecular Biology.

(1) (a) Lindskog, S.; Engberg, P.; Forsman, C.; Ibrahim, S. A.; Johnson, B. H.; Simonsson, I.; Tibell, L. *Ann. N.Y. Acad. Sci.* **1984**, *429*, 61. (b) Lindskog, S. In *Zinc Enzymes*; Bertini, I., Luchinat, C., Maret, W., Zeppezauer, M., Eds.; Birkhäuser: Boston, 1986; 307-316.
(2) Bertini, I.; Luchinat, C.; Scozzafava, A. *Structure Bonding* **1982**, *48*, 46.
(3) Silverman, D. N.; Vincent, S. H. *CRC Crit. Rev. Biochem.* **1983**, *14*, 207.
(4) Silverman, D. N.; Lindskog, S. *Acc. Chem. Res.* **1988**, *21*, 30.
(5) Cook, C. M.; Haydock, K.; Lee, R. H.; Allen, L. C. *J. Phys. Chem.* **1984**, *88*, 4875.
(6) Demoulin, D.; Pullman, A. *Theor. Chim. Acta* **1978**, *49*, 161.
(7) Pullman, A.; Demoulin, D. *Int. J. Quantum. Chem.* **1979**, *16*, 641.
(8) Pullman, A. *Ann. N.Y. Acad. Sci.* **1981**, *367*, 340.
(9) (a) Liang, J. Y.; Lipscomb, W. N. *Biochemistry* **1987**, *26*, 5293. (b) Liang, J. Y.; Lipscomb, W. N. *Biochemistry* **1988**, *27*, 8676.
(10) Liang, J. Y.; Lipscomb, W. N. In *Sixth Conversation in Biomolecular Stereodynamics*; Sarma, R. H., Ed.; 1989; p 204.

0002-7863/90/1512-8692$02.50/0

by using eigenvalues and eigenvectors obtained from diagonalization of the Hessian matrices. It is the purpose of this work to overcome these limitations.

Particular attention is given to the characterization of first-order saddle points (transition structures, TSs); such structures gate well-defined molecular rearrangements when the two directions of the transition vector (TV) are followed in the internal coordinate space with the help of energy minimization procedures; these changes are well defined and may be related to experimentally based molecular mechanism.[11-14] An effort is made, via molecular docking of stationary structures onto the X-ray structures of various CAs, to provide theoretical hints to help understand microreversibility and differential kinetic behavior in carbonic anhydrases (CAs).

As a first step in establishing the roles zinc cation may have in the interconversion reaction, bare zinc reactive complexes, namely, $[ZnOHCO_2]^+$ and $[ZnHCO_3H_2O]^+$, have been studied. Thereafter, and to move the discussion toward the properties of zinc when it is at the active site of CAs, ammonia molecules have been used to mimick N-atom binding provided by the three histidines; ammonia molecules have been successfully employed by other authors[7,8] to model such bonds. Electronic properties of $[Zn(NH_3)_3OH]^+$ and $[Zn(NH_3)_3OH_2]^{2+}$ and sections of the hypersurface for $[Zn(NH_3)_3OCOOH]^+$ have been calculated at the same high basis set level as for bare zinc complexes.

There is a general interest in knowing how much of the catalytic properties might be due to the metal and what contributions the coordination shell can be credited for. Such information might be valuable in tailoring model enzymes systems.[15] For bare zinc complexes, this paper focus on two mechanistic issues: (i) elucidation of the role zinc ion may have on the reaction pathways leading to carbon dioxide hydration and bicarbonate dehydration in vacuo and (ii) discrete solvation effects on bicarbonate binding. The energy hypersurface of $[ZnOHCO_2]^+$ has been searched; three scenarios related to some general mechanistic issues are described in Scheme I: (i) a nucleophilic attack of zinc-bound hydroxyl group onto carbon dioxide (case I); (ii) a carbonyl activation by zinc (case II); and (iii) nucleophilic attack plus a carbonyl activation either by zinc (case III) or by the hydroxyl proton (case IV). Three TSs have been obtained at a RHF-SCF level which can be considered as illustrations of cases II-IV. The details of these calculations are examined in section III.

Active and passive displacement solvation effects of one water molecule on monodentate zinc-bound bicarbonate TS have been studied for the $[ZnHCO_3H_2O]^+$ molecular model. Interestingly, the energy profile including reactants $[ZnOH^+ + CO_2]$ and products $[Zn^{2+} + HCO_3^-]$ that goes through the interconversion TS and the monodentate bicarbonate saddle point has an inverted shape,[16,17] i.e., the energy level of the transition structures found along the reactive path are all below the energy levels of the reactant and/or the product. The inclusion of correlation energy calculated at each SCF stationary point of the hypersurface at a MP2 level does not change the fundamental results obtained with the HF scheme. The results are presented with a discussion on their relevance to the molecular mechanism in section IV.

The studies of ammonia liganded complexes permit comparisons with bare zinc calculations on the following issues: (i) zinc hydroxide nucleophilicity; (ii) bicarbonate/water exchange energy balance; (iii) characterization of the monodentate bicarbonate binding structure on the energy hypersurface spanned by the full set of geometrical variables, followed by an exploration of the resulting transition vector; and (iv) pyramidal and tetrahedral coordination models of zinc cation. One important point documented here is the conserved saddle point character of bicarbonate monodentate binding to zinc; this result emphasizes the major contribution of zinc itself. The energy profile leading to interconversion conserves its inverted nature. In section V results are presented and discussed.

Scheme I

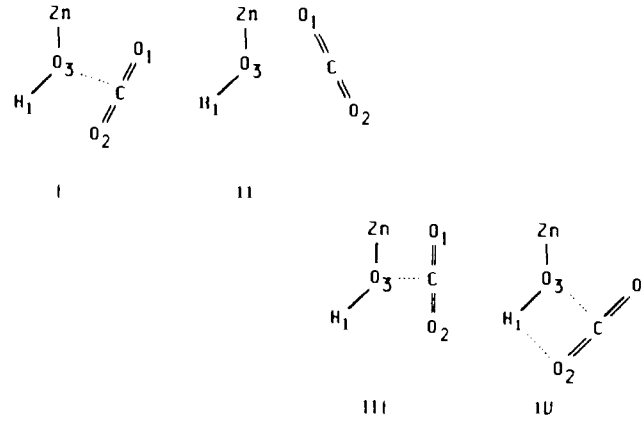

In section VI the tenets of the catalytic mechanism currently accepted for human carbonic anhydrase II (HCAII) are discussed in light of our theoretical results. Although the ab initio calculations correspond to gas-phase systems, the electronic factors are likely to be robust features which will probably be operating at the enzyme level. Differences at the active sites level of human CAI and bovine CAIII are examined.

In section VII, previous theoretical works are discussed as well as the numerous mechanistic proposals that are acknowledged. Conclusions and perspectives are discussed there.

II. Methods and Models

(i) **Materials and Methods.** The calculations have been performed with the programs MONSTERGAUSS[18a] for the optimizations and GAUSSIAN-86[18b] for the analytic force constant matrix estimations. Stationary points on the energy hypersurfaces have been located with the VA05 subroutine of Powel,[19] and descents along the transition vectors have been made with the conjugate gradient method of Davidon.[20] Alliants FX-40 and FX-80 have been used to perform the calculations.

The Zn basis set consisted on the (14s,9p,5d) primitive Gaussian functions reported by Watcher[21] and contracted to (6,2,2,2,1,1/6,1,2/3,2) by Clementi and co-workers.[22] For O, N, and C, the (9s,5p) basis sets of Van Duijneveldt[23] contracted to (5,2,1,1/3,2) by Clementi[22] have been used. For hydrogen, a 4s basis set with a (3,1) contraction is used.[24]

Bond orders and net atomic charges have been obtained from standard population analysis techniques.[25] Correlation energy has been estimated by using the perturbative approach based on Møller-Plesset zero-order Hamiltonian.[26] Only diexcitations have been taken into account and these for the smaller model systems only.

Molecular dockings have been made by using FRODO[27] implemented

(11) McIver, J. W. *Acc. Chem. Res.* **1974**, *7*, 72.
(12) Truhlar, D. G.; Hase, W. L.; Hynes, J. T. *J. Phys. Chem.* **1983**, *87*, 2664.
(13) Pauling, L. *Nature (London)* **1948**, *161*, 707.
(14) (a) Tapia, O.; Cardenas, R.; Andres, J.; Colonna-Cesari, F. *J. Am. Chem. Soc.* **1988**, *110*, 4046. (b) Andres, J.; Cardenas, R.; Silla, E.; Tapia, O. *J. Am. Chem. Soc.* **1988**, *110*, 666. (c) Tapia, O.; Lluch, J. M.; Cardenas, R.; Andres, J. *J. Am. Chem. Soc.* **1989**, *111*, 829.
(15) (a) Krechl, J.; Castulik, P. *Chem. Scr.* **1989**, *29*, 173. (b) Tabushi, I.; Kuroda, Y. *J. Am. Chem. Soc.* **1984**, *106*, 4580.
(16) (a) Cao, H. Z.; Allavena, M.; Tapia, O.; Evleth, E. M. *Chem. Phys. Lett.* **1983**, *96*, 458. (b) Cao, H. Z.; Allavena, M.; Tapia, O.; Evleth, E. M. *J. Phys. Chem.* **1985**, *89*, 1581.
(17) Olmstead, W. N.; Brauman, J. I. *J. Am. Chem. Soc.* **1977**, *99*, 4219.
(18) (a) Program MONSTERGAUSS: Peterson, M. R.; Poirier, R. A. University of Toronto, Ontario, Canada, 1980. (b) Program GAUSSIAN-86: Frisch, M. J.; Binkley, J. S.; Schlegel, H. B.; Raghavachari, K.; Melius, C. F.; Martin, R. L.; Stewart, J. J. P.; Bobrowicz, F. W.; Rohlfing, C. M.; Kahn, L. R.; Defrees, D. J.; Seeger, R.; Whiteside, R. A.; Fox, D. J.; Fleuder, E. M.; Pople, J. A. Carnegie-Mellon Quantum Publishing Unit: Pittsburgh, PA, 1984.
(19) Powel, M. J. D. Atomic Energy Research Establishment, Harwell, U.K.
(20) Davidon, W. C. *Mathematical Programming* **1975**, *9*, 1.
(21) Watchers, A. J. H. *J. Chem. Phys.* **1970**, *52*, 1033.
(22) Gianolo, L.; Pavani, R.; Clementi, E. *Gazz. Chim. Ital.* **1978**, *108*, 181.
(23) Van Duijneveldt, F. 1.B.M. Technical Report RJ945, Dec 1971.
(24) Exponents for the 1s contraction are 26.972837, 4.0685679, and 0.92177523 with coefficients 0.0033494, 0.23472695, and 0.81375733; the exponent for the 2s orbital is 0.21328984. Scale factors of 1.2 and 1.15 were used for the 1s and 2s orbitals, respectively.
(25) Mayer, 1. *Chem. Phys. Lett.* **1983**, *97*, 270.
(26) Binkley, J. S.; Pople, J. A. *Int. J. Quant. Chem.* **1975**, *9*, 229.
(27) Jones, T. A. *J. Appl. Crystallogr.* **1978**, *11*, 268.

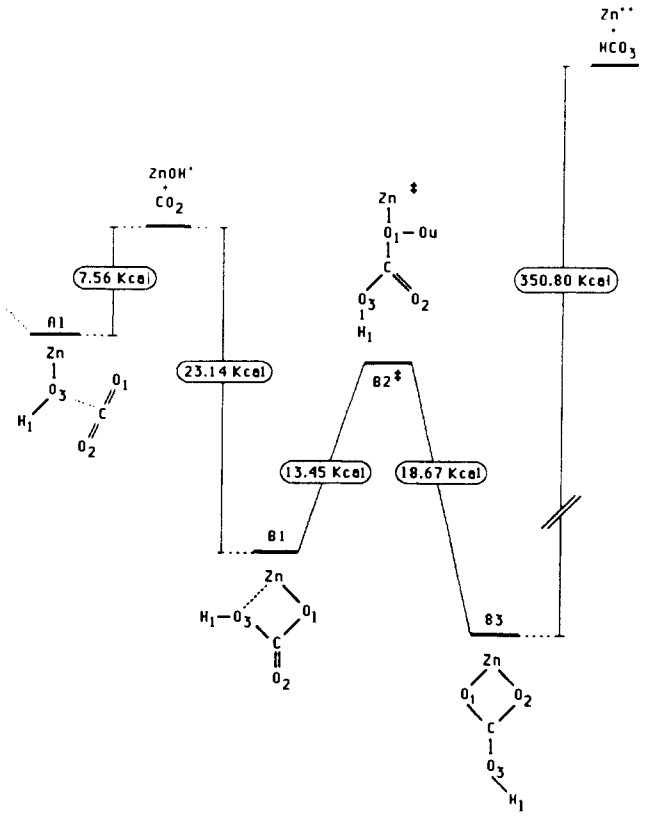

Figure 1. Schematic in vacuo SCF energy profile representing the simple nucleophilic attack of zinc-bound hydroxide on carbon dioxide (path A) and the possible modes of bicarbonate binding to zinc (path **B**). **B2** is a transition structure, calculated over the full internal geometry space, describing a rotation of the bicarbonate moiety between mono- and bidentate complexed forms. **B1** and **B3** are its related minima. Du is a dummy atom used for the definition of **B2**. The dummy atom is fixed to the bicarbonate frame (CO1Du = 90°).

for an Evans & Sutherland PS390 display and a Silicon Graphics PERSONAL-IRIS. Coordinates for native carbonic anhydrases were obtained from the Brookhaven Data Bank[28] for the HCAI[29] and from Eriksson et al. for HCAII[30] and BCAIII.[31]

(ii) **Searches on the Energy Hypersurfaces.** The energy hypersurface in vacuo has an inverted shape with respect to the partners [$ZnOH^+$ + CO_2] and [Zn^{2+} + HCO_3^-]. This is also true for [$Zn(NH_3)_3HCO_3$]$^+$ and [$ZnHCO_3H_2O$]$^+$ hypersurfaces. This means that the stationary points along the reactive path are all at the bottom of a well. This feature makes the search after saddle points extremely difficult. The techniques used to bracket them have been already described by us.[14,32]

Stationary points are characterized after diagonalizing the Hessian matrix (force constant matrix in internal coordinates). For a minimum, all eigenvalues are positive, a TS is a first-order saddle point calculated over the whole hypersurface. Higher order saddle points have also been found. To determine a reaction path, descents from the corresponding TS along the directions defined by the transition vectors (TV) are made which permit connecting related minima on the hypersurface.[14,33-35] The study of alternative pathways requires a characterization of all (if possible) saddle points related to the corresponding mechanistic proposals.

(iii) **Models.** Structural and energetic data of water, hydroxyl ion, and other partners entering in the model hypersurfaces are reported in Table I. Energies, gradients, equilibrium geometric parameters, force constants are given at RHF-SCF level and for nonliganded complexes energies are reported at an RHF-SCF-MP2 level.

Force constants for carbon dioxide and water derived from experiment are given in Table I. A comparison between theoretical and experimental values shows an excellent agreement. As one would expect, SCF force constants are slightly overvalued.

Atom labels and numbering used throughout the discussions are indicated in Table I, Scheme I, and figures.

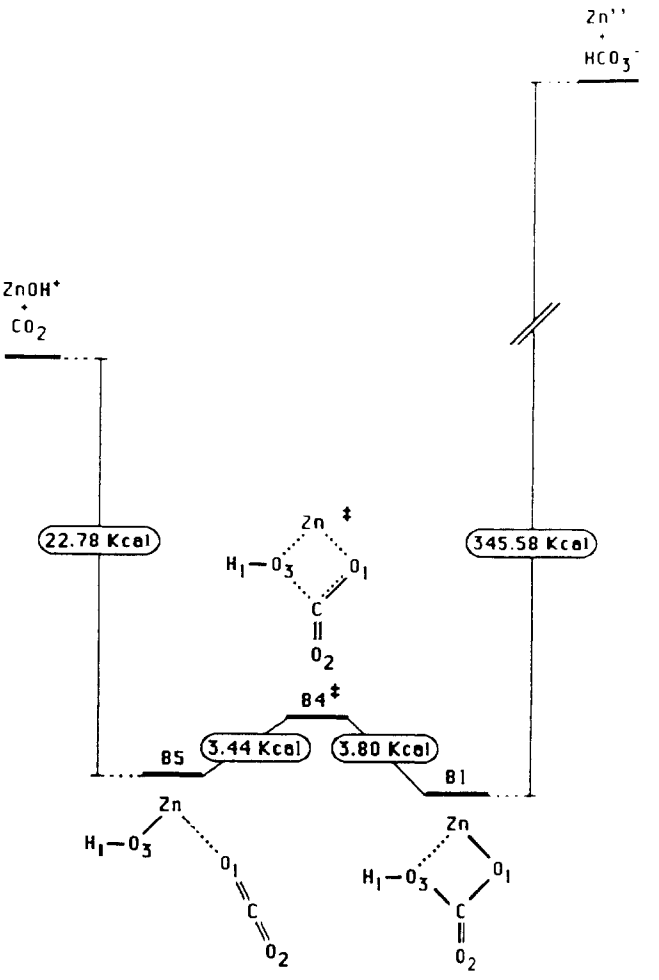

Figure 2. Schematic in vacuo SCF energy profile describing the carbon dioxide/bicarbonate interconversion process. **B4** is a first-order saddle point over the full internal coordinate space; **B5** and **B1** are its related minima.

III. CO_2/HCO_3^- Interconversion; $[ZnOHCO_2]^+$ Hypersurface

In absence of zinc the CO_2 hydroxylation in vacuo is barrierless and 99 Kcal/mol exothermic as shown by the entries of Table I; similar results have been found by other authors.[36-38]

Including zinc and taking the stationary structure of lowest energy on this hypersurface, which describes a zinc-bound bicarbonate (cf. Figure 1), a drastic reduction of 71 Kcal/mol in exothermicity is obtained. Note that by measuring the energy difference with respect to the separate ionic species [Zn^{2+} + HCO_3^-] the reaction becomes endothermic.

Thus, zinc cation profoundly modifies the global energetics of carbon dioxide hydroxylation reaction in vacuo.

The hypersurface has [$ZnOH^+$ + CO_2] as reactants and [Zn^{2+} + HCO_3^-] as products. Calculations are carried out from both sides with the following objectives: (i) to test direct nucleophilic attack of $ZnOH^+$ onto CO_2 (alternative I in Scheme I); and (ii) to examine bicarbonate binding to Zn^{2+}. Results are summarized in Figures 1 and 2 and Tables I–V.

(28) Berstein, R. *J. Mol. Biol.* **1977**, *112*, 535.
(29) Kannan, K. K.; Ramanadham, M.; Jones, T. A. *Ann. N.Y. Acad. Sci.* **1984**, *429*, 49.
(30) Eriksson, E. A.; Jones, T. A.; Liljas, A. *Proteins* **1988**, *4*, 274.
(31) Eriksson, E. A. Thesis, Uppsala University, 1989.
(32) Tapia, O.; Andres, J. *Chem. Phys. Lett.* **1984**, *109*, 471.
(33) Williams, I. A.; Spangler, D.; Femec, D. A.; Maggiora, G. M.; Schowen, R. L. *J. Am. Chem. Soc.* **1983**, *105*, 31.
(34) Schlegel, H. B. In *Ab Initio Methods in Quantum Chemistry*; Lawley, K. P., Ed.; 1987; p 250.
(35) *Transition States of Biochemical Processes*; Gandour, R. D., Schowen, R. L. Eds.; Plenum Press: New York, 1978.
(36) Jonsson, B.; Karlstrom, G.; Wennerstrom, H. *J. Am. Chem. Soc.* **1978**, *100*, 1658.
(37) Jonsson, B.; Karlstrom, G.; Wennerstrom, H.; Forsen, S.; Roos, B.; Almlof, J. *J. Am. Chem. Soc.* **1977**, *99*, 4628.
(38) Liang, J. Y.; Lipscomb, W. N. *J. Am. Chem. Soc.* **1986**, *108*, 5051.

Table I. Energetic and Structural Data Accounting for the Partners Entering the Different Hypersurfaces Reported in This Study[a]

structure	SCF energy (au) MP2 energy)	gradient length (mdyne)	optimized geometry (Å, deg) (force constant (mdyne/Å))
OH^-	−75.300 912 (−75.403 867)	1.72×10^{-5}	OH = 0.999 (5.72)
OH_2	−75.998 642 (−76.113 693)	1.09×10^{-4}	OH = 0.951 (8.96, 8.45[a]), HOH = 110.7 (0.78, 0.70[a])
CO_2	−187.502 126 (−187.850 503)	1.03×10^{-4}	CO = 1.170 (18.9[b] 16.02[a]), OCO = 180.0 (1.00,[b] 0.78[a])
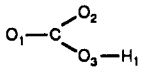	−262.960 880 (−263.391 778)	1.90×10^{-4}	CO1 = 1.238 (11.25), CO2 = 1.250 (10.43), CO3 = 1.446 (4.34), O3H1 = 0.952 (8.85), O3CO1 = 114.8 (3.01), O3CO2 = 113.1 (3.36), CO3H1 = 106.7 (0.81)
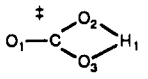	−262.894 512 (−263.343 411)	3.98×10^{-4}	CO1 = 1.229 (11.93), CO2 = CO3 = 1.354 (5.96), O3H1 = 1.256 (−0.84), O1CO2 = 129.8 (2.43), O2CO3 = 100.3 (3.61), CO3H1 = 740 (2.42)
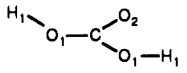	−263.519 603 (−263.952 879)	2.09×10^{-4}	CO1 = 1.339 (7.44), CO2 = 1.209 (13.45), O1CO2 = 125.0 (2.85), CO1H1 = 114.0 (0.80), O1H1 = 0.952 (8.93)
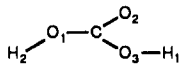	−263.519 815 (−263.953 601)	2.31×10^{-4}	CO1 = 1.340 (7.52), CO2 = 1.201 (4.08), CO3 = 1.357 (6.83), O3H1 = 0.951 (9.12); O1H2 = 0.952 (9.04), O2CO1 = 125.0 (2.88), O2CO3 = 124.5 (3.04), CO1H2 = 115.2 (0.78), CO3H1 = 114.7 (0.76)
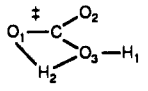	−263.428 169 (−263.888 323)	5.95×10^{-4}	CO1 = 1.281 (8.41), CO2 = 1.185 (14.59), CO3 = 1.569 (1.46), O3H1 = 0.945 (9.48), O3H2 = 1.184 (−0.203), O2CO1 = 144.7 (4.43), O2CO3 = 123.5 (3.79), CO3H2 = 74.6 (1.61), CO3H1 = 134.2 (0.50)
Zn^{2+}	−1776.717 508 (−1776.906 301)		
$ZnOH^+$	−1852.690 103 (−1853.006 338)	2.79×10^{-4}	ZnO = 1.777 (3.85), OH = 0.953 (8.89), ZnOH = 124.6 (0.43)
$ZnOH_2^{2+}$	−1852.871 768 (−1853.177 677)	2.43×10^{-4}	ZnO = 1.872 (2.64), OH = 0.961 (8.57), ZnOH = 125.8 (0.76), HOH = 108.4 (1.14)
$Zn^{2+}(NH_3)_3Du$[c]	−1945.659 844	1.57×10^{-4}	ZnN = 2.007, NH = 1.010, NZnDu = 90.3, ZnNHe = 113.3, ZnNHa = 113.0
$Zn(NH_3)_3OH^+$	−2021.416 596	1.68×10^{-4}	ZnN = 2.110, ZnO = 1.759, OH = 0.931, NHa = 1.003, NHe = 1.005,[c] ZnOH = 180.0, OZnN = 112.5, ZnNHa = 119.3, ZnNHe = 106.8
$Zn(NH_3)_3OH_2^{2+}$	−2021.725 209	3.84×10^{-4}	ZnN = 2.052, ZnO = 2.0518 OH = 0.953, NH = 1.008, ZnOH = 125.7, HOH = 108.6, OZnN = 105.3, ZnNH = 112.8
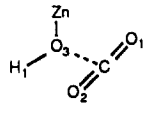 **A1**	−2040.204 271 (−2040.864 210)	2.38×10^{-4}[d]	ZnO3 = 1.771 (4.09), O3H1 = 0.951 (8.97), CO3 = 2.500 (0.25), CO1 = 1.177 (15.59), CO2 = 1.164 (14.13), ZnO3H1 = 125.8 (0.46), ZnO3C = 117.7 (−0.10), O3CO1 = 83.2 (0.97), O3CO2 = 100.3 (0.62)

[a] Experimental force constants values derived from Mills, I. M. In *Theoretical Chemistry*; Quantum Chemistry, Specialist Periodical Report, Vol 1, pp 110–159. [b] Numerical force constant. [c] Du is a dummy atom. [d] CO3 = 2.5 Å with residual gradient of 0.007 mdynes, and ZnO3C = 117.7° with residual gradient of 0.102 mdynes.

Zn–OH$^+$ Nucleophilicity. The nucleophilic power of OH^- bound to zinc is also drastically modified. This effect can be elicited by scanning the interaction path starting from the geometry-optimized reactants and approaching along the CO3 axis in a symmetric disposition with respect to the ZnO3H1 angle. In this manner, the possibility of carbonyl activation by zinc or by the hydroxyl proton is reduced as the corresponding interatomic distances are maximized. An energy minimum was found at 2.5 Å. A constrained stationary point **A1** results from a geometry optimization of this complex by fixing CO3 distance (2.5 Å) and ZnO3C angle (117.7°). In Figure 1 the structure is depicted. The whole space Hessian matrix is calculated at this point and diagonalized. Structure **A1** is a first-order saddle point: the variable ZnO3C has a negative force constant and controls the TV (cf. Table I); by moving along the transition vector directions one would reach the structures accounting for cases III and IV in Scheme I, i.e., activation of carbonyl either by zinc or hydroxyl proton.

The present results show that nucleophilicity, as defined in refs 1,4,6–8,9b which qualify the ability of the bound hydroxide to perform a nucleophilic attack on carbon dioxide, is inhibited by interactions with bare zinc cation. Such results concern gas-phase events.

Zinc Bicarbonate Binding. An energy scan using Zn···O1 distance along the bond direction CO1 of bicarbonate was made with all atoms in the same plane. Starting from the minimum energy structure a second-order saddle point is characterized. By moving zinc and the hydrogen atom out of the plane in an antisymmetric form, a first-order saddle point is obtained. This one is described by structure **B2** in Figure 1. In Table II relative energies, force constants, and geometric entries are reported for

Table II. Geometries (Å and deg), Force Constants (mdyn/Å), and Transition Vector for the Stationary Points Describing the Different Modes of Bicarbonate Binding to Zinc[a]

	B1		**B2**‡			**B3**	
	geom	*K*	geom	*K*	C1	geom	*K*
ZnO1	1.865	3.39	1.745	4.51	0.00	1.961	2.61
ZnO2			3.713			1.969	
ZnO3	2.010		3.643				
CO1	1.303	8.11	1.326	7.78	0.00	1.283	8.97
CO2	1.189	14.61	1.204	13.92	0.01	1.293	8.15
CO3	1.494	3.37	1.348	7.12	−0.02	1.305	8.54
H1O3	0.950	9.22	0.953	9.21	0.00	0.956	8.68
ZnO1C	100.7	3.47				89.7	5.45
ZnO1Du			88.0	−0.13	−1.00		
O1CO2	136.8	2.23	124.5	2.85	−0.02	114.4	5.79
O1CO3	102.6	6.13	110.9	3.03	0.01	122.1	2.36
CO3H1	115.8	0.78	115.4	0.78	−0.01	118.2	0.74
O3CO1O2	180.0	0.87	181.0	0.55	−0.06	180.0	0.53
H1O3CO1	180.0	0.20	186.5	0.15	0.02	180.0	0.15
ZnO1DuC			213.5	0.15	−0.01		
ZnO1CO2	180.0	0.50				0.0	0.78

[a] The SCF and MP2 energies (au) and the gradient lengths (mdyn) are −2040.229 103, −2040.866 816, and 1.93×10^{-4} for **B1**; −2040.207 674, −2040.831 934, and 8.93×10^{-5} for **B2**; −2040.237 420, −2040.867 735, and 3.96×10^{-4} for **B3**. The unique negative eigenvalue of **B2** is −0.137 mdyn/Å. Du is a dummy atom; CO1Du is fixed to 90°.

Table III. Bond Orders Accounting for the Zinc Bicarbonate Moiety in the Stationary Structures Described in This Study[a]

code	ZnO1	ZnO2	ZnO3	CO1	CO2	CO3	H1O3
A1	0.00	0.00	0.66	1.73	1.85	0.05	0.74
B1	0.33	0.00	0.12	1.14	1.82	0.69	0.66
B2‡	0.42	0.05	0.01	0.99	1.74	0.94	0.68
B3	0.25	0.24	0.00	1.31	1.27	1.05	0.65
B4‡	0.14	0.00	0.32	1.37	1.92	0.35	0.71
B5	0.05	0.00	0.57	1.57	1.98	0.01	0.76
B6‡	0.24	0.00	0.20	1.31	1.37	0.95	0.31
C1c	0.28	0.00	0.00	1.05	1.73	0.89	0.69
C2c‡	0.13	0.00	0.00	0.91	1.78	0.95	0.67
C3c	0.07	0.00	0.00	0.83	1.82	0.99	0.65
B1T	0.17	0.00	0.01	1.17	1.69	0.82	0.70
B1P	0.15	0.00	0.05	1.24	1.70	0.74	0.70
B2T‡	0.13	0.01	0.01	1.17	1.65	0.87	0.71
B3T	0.14	0.01	0.00	1.18	1.61	0.90	0.71
B3P	0.11	0.11	0.00	1.38	1.33	0.96	0.68
HCO_3^-				1.46	1.53	0.76	0.78

[a] Bond orders for OH^-, H_2O, and CO_2 are 0.95, 0.77, and 1.81, respectively. In the liganded complexes, ZnN and NHBO are about 0.13 and 0.77.

B2 and its related minima **B1**, and **B3** is calculated over the full internal geometric space.

The TS-**B2** can be seen as containing a perturbed bicarbonate ion. Comparing its force constants with free bicarbonate shows that the carbon dioxide moiety is asymmetrically affected: the force constant (in units of mdyn/Å) of CO2 bond increases from 10.4 to 13.9 indicating the presence of a double bond; the CO1 force constant decreases from 11.3 down to 7.8 which is better described as a single CO bond. Note that the force constants for the double and single CO bond in carbon dioxide and carbonic acid are about 19 and 17, respectively (cf. Table I). The OC force constant, for the hydroxyl moiety bound to carbon dioxide, increases from 4.3 to 7.1.

The TV is controlled by only one variable (ZnO1Du), with a negative force constant (−0.06) describing a rotation of bicarbonate between monodentate and bidentate complexed forms (see Figure 1). The saddle point nature does not depend upon the definition of the dummy atom;[39] this representation has been retained for the sake of comparisons with the liganded complexes; moreover, the dummy atom eliminates accidental linearities of the bond system with ligands. The TV displacement is not coupled to the rest of the geometrical variables in the neighborhood of the stationary point. Note, however, that the internal geometry of bicarbonate and the force constant system change as one moves along the TV.

The bidentate planar complex **B3** is 19 Kcal/mol below the TS. This is the lowest energy minima characterized on this hypersurface. The bond system in the bicarbonate moiety shows a set of well-defined CO single bonds with a force constant of 8.5 mdynes/Å. A comparison of **B3** with free bicarbonate shows that the CO3 bond becomes stiffer in the former structure.

The descent along the direction opposite to **B3** leads to the minimum energy structure **B1** which is 13 Kcal/mol below the TS. The monodentate bicarbonate form in structure **B2** is changed into an intermediate planar coordination structure in **B1** somewhere in between mono- and bidentate binding states (ZnO1 = 1.86 and ZnO3 = 2.01 Å).

The force constants of **B1** compared to **B2** for the carbon dioxide moiety have not significantly changed. On the contrary, the force constant for the CO3 bond describing the relative displacement of the hydroxide and carbon dioxide moieties has been lowered from 7.1 to 3.4. The ZnO1 force constant slightly decreases, while the interatomic distance changes from 1.74 to 1.86 Å. This bond distance shift reflects the engagement of zinc in a new bond-like interaction.

The bond orders (BOs) for all these structures are given in Table III. The carbon dioxide moiety BOs reflect electronic rearrangements due to zinc binding. Complex **B3** corresponds to a bicarbonate electronic structure slightly modified by zinc. On the contrary, the **B2** and **B1** complexes present a CO2 double bond reminiscent of the carbon dioxide structure. The CO3 BO steadily decreases from 1.0 in **B3** to 0.7 in **B1** indicating a weakening of the interaction between carbon dioxide and OH moieties. Therefore, the passage from **B3** to **B1** is not only a simple rotation, but it involves a weakening of the incumbent bond during the dehydration reaction and the formation of a CO double bond prefigurating carbon dioxide.

Table IV. Geometries (Å and deg), Force Constants (mdynes/Å), and Transition Vector for the Stationary Points Describing the Carbon Dioxide/Bicarbonate Interconversion Process[a]

	B4‡			**B5**	
	geom	*K*	C1	geom	*K*
ZnO1	1.985	1.84	0.20	2.086	0.79
ZnO3	1.817			1.768	4.22
CO1	1.231	12.98	−0.08	1.186	14.23
CO2	1.161	16.23	−0.03	1.151	16.93
CO3	1.922	1.02	0.74		
H1O3	0.944	9.54	−0.01	0.946	9.28
ZnO1C	104.8	12.31	0.21	140.9	0.09
O1CO2	154.3	1.44	0.45	178.1	1.05
O1CO3	92.4	14.89	−0.28	57.2	
H1O3C	123.7	0.45	0.29	155.0	
ZnO3H1	149.5			133.0	0.36
O32NO1	76.0			90.0	0.28
ZnO1CO2	180.0	0.59	0.00	180.0	
O3CO1O2	180.0	0.72	0.00	180.0	
H1O3CO1	180.0	0.12	0.00	180.0	

[a] The SCF and MP2 energies (au) and the gradient lengths (mdynes) are −2040.223 055, −2040.871 252, and 1.32×10^{-4} for **B4**; −2040.228 539, −2040.879 737, and 1.91×10^{-4} for **B5**. The unique negative eigenvalue of **B4** is −0.18 mdyn/Å. O3ZnO1 = 90° for **B5**.

Monodentate bicarbonate binding to zinc via hydroxyl oxygen (O3) does not exist on the present hypersurface. All trials have ended by converging toward **B1**. This result is not surprising since this complex has an energy above the reactant limit $ZnOH^+ + CO_2$, and the nucleophilic power of the zinc-bound hydroxide is almost nonexistent.

The electronic structure of zinc-bound bicarbonate **B2** does not give any direct hints concerning carbon–oxygen bond breaking which would correspond to the dehydration process, while structure **B1** does contain them. However, this point does not have a saddle point character and, therefore, does not qualify to represent an interconversion process. Now, if one analyzes different eigenvectors in **B1**, which were obtained after Hessian diagonalization, there is one moving the system upwards to **B2** with an eigenvalue equal to 1.3 (in units of mdyn/Å) and a second one with an eigenvalue equal to 0.69 that shows an antisymmetric motion describing a displacement of O1 away from zinc, a break of the CO3 bond, a shortening of the ZnO3 distance, and an increase of the O1CO2 angle. This eigenvector is used to explore the hypersurface.

CO_2/HCO_3^- Interconversion. A first-order saddle point **B4** has been characterized at about 4 Kcal/mol above **B1**. Its schematic structure is shown in Figure 2. In Table IV the diagonal force constants and the eigenvector corresponding to the unique negative eigenvalue are reported.

The structure of **B4** is compared to **B1**. The carbon dioxide moiety which is a virtual object in **B1** acquires a real presence in **B4**. The O1CO2 angle and force constant change from 137° and 2.2 mdynÅ/rad to 154° and 1.4 mdynÅ/rad in the TS thereby approaching the 1.0 mdynÅ/rad for carbon dioxide. The force constant of the CO1 bond which is 8.1 in **B1** increases to 13 in **B4**; bond orders change in the same manner: from 1.1 to 1.4. Free carbon dioxide has an CO force constant of 18.9 which is comparable to the values of **B4**, namely 13 and 16. These results show that the O1CO2 moiety actually corresponds to a bent carbon dioxide.

The hydroxyl moiety acquires a definite presence in the TS. It is bound to zinc at variance with complex **B1**; the BO increases from 0.1 up to 0.3, and the ZnO3 distance decreases from 2 to 1.8 Å. The bond between zinc and O1 weakens significantly; the force constant in **B1** is twice as strong as in **B4**. Around zinc,

Table V. Geometry (Å and deg), Force Constants (mdynes/Å), and Transition Vector for the Stationary Structure Describing the Intramolecular Proton Transfer between **B1** and **B3**[a]

	B6‡		
	geom	*K*	C1
ZnO1	1.985		
ZnO3	1.962	2.34	0.04
CO1	1.271	8.86	0.06
CO2	1.267	9.75	−0.16
CO3	1.384	5.18	0.31
H1O3	1.287	−0.96	−0.69
H1O2	1.347		
ZnO3C	88.1	5.09	−0.04
O1CO2	142.7	4.67	0.04
O2CO3	104.0	3.76	0.38
CO3H1	74.6	0.96	0.49
ZnO3CO2	180.0	0.65	0.00
O1CO2O3	180.0	0.44	0.00
H1O3CO2	0.0	1.19	0.00

[a] SCF and MP2 energies (au) and gradient length (mdyn) are −2040.132 686, −2040.786 305, and 7.88 × 10^{-5}, respectively. The unique negative eigenvalue of **B6** is −7.01 mdyn/Å.

a bond is broken, and another is simultaneously formed along the reaction path connecting **B1** to **B4**. Concurrently, two bonds and the bond angle are changed in the bicarbonate moiety. One is the CO1 bond which moves from single to double, and the other is the CO3 bond which is significantly weakened; the interatomic distance CO3 moves from 1.5 to 1.9 Å; the force constant changes from 3.4 to 1.0 and the BO from 0.7 to 0.35 showing that there remains electronic interactions although the bond is being clearly broken.

The saddle point **B4** describes a four-center interaction complex between a deformed carbon dioxide and zinc-bound hydroxyl moieties. It represents a real nucleophilic attack by zinc-bound hydroxide ion onto a carbon dioxide *whose carbonyl function has been activated by zinc.*

The structure of the TV reflects this four-bond four-center interaction process (cf. Table IV). Along one direction one descends toward **B1** (bicarbonate), while along the opposite direction carbon dioxide is formed. The bond CO3 breaks, and the Zn–carbon dioxide bond weakens. The structure **B5** in Figure 2 is a point on the energy hypersurface found at 3.4 Kcal/mol below **B4**. The angle O3ZnO1 has a value of 90° with a weak repulsive gradient (−0.07 mdynes-Å/rad); the remaining parameters are optimized with a gradient length of 1.9 × 10^{-4} mdynes. At this point the Hessian is calculated over the full internal space. The point has one negative eigenvalue (−0.075), and it is symmetrically controlled by O3ZnO1 (amplitude 0.81 in TV) and ZnO1C (0.57). The structure of the hypersurface around **B5** shows the difficulties faced to reach **B4** starting from ZnOH plus carbon dioxide using standard search algorithms.

B5 describes a weak interaction of carbon dioxide with zinc. ZnO1 force constant changes from 1.8 in **B4** to 0.8 in **B5**; BOs are 0.14 and 0.05, respectively. BO for ZnO3 increases from 0.3 to 0.6.

From a mechanistic point of view, the pathway **B5–B4–B1** represents the interconversion process between carbon dioxide and bicarbonate in vacuo. In view of the energetics displayed in Figure 2, this process should be reversible with a small activation energy if all molecular rearrangements were to take place at the bottom of the well. Structures **B5** and **B4** correspond to cases II and III in Scheme I, respectively.

The roles played by bare zinc in the carbon dioxide hydroxylation can be summarized now: (i) inhibition of simple hydroxide nucleophilicity strength; (ii) carbon dioxide carbonyl activation; and (iii) well-defined interconversion pathway at the bottom of an inverted energy profile with low activation barrier.

Intramolecular Proton Transfer. The structure **B1** is in the crossway of two important paths, one toward **B5** (carbon dioxide binding) and the other toward **B3** (bidentate bicarbonate binding) as indicated in Figures 1 and 2. Nonetheless, there is another way to change **B1** into **B3** which goes over a direct proton transfer

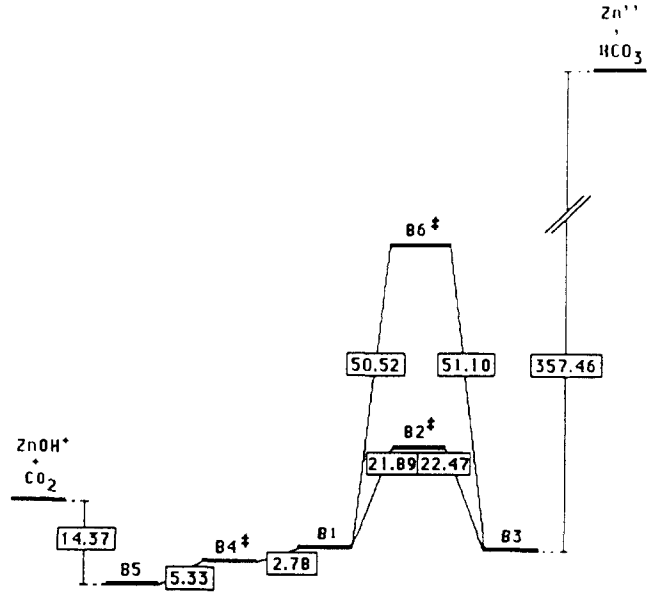

Figure 3. Schematic energy diagram representing the SCF–MP2 energy calculations for the stationary structures of the $[ZnOHCO_2]^+$ hypersurface. No geometry optimization has been attempted.

from O3 to O2. This is an internal proton transfer of a zinc-bound bicarbonate similar to the one discussed by Liang and Lipscomb.[9a] A transition structure **B6** has been characterized and is described in Table V.

B6 has a clear bidentate structure resembling **B3** with bond orders 0.20 and 0.24 compared to 0.25 and 0.24 in **B3**. Zn oxygen distances and CO bond force constants for **B3** and **B6** are quite comparable.

In Table I the transition structure for the intramolecular proton transfer in absence of zinc is given; the transition vectors with and without metal are identical. The activation barrier for the system without zinc amounts to 42 Kcal/mol, whereas it increases to 66 Kcal/mol if one measures it from **B3**. It is apparent that zinc binding does not facilitate this intramolecular proton transfer.

An eventual TS associated to an intramolecular proton transfer starting from the monodentate binding of zinc onto O3 has been searched. All attempts have ended converging to **B6**. One can presume that if such a structure exists it should be located well above **B6** on the energy hypersurface. Actually such a structure would have a related minima zinc bound to the monodentate bicarbonate at O3 (hydroxyl moiety) and **B2**. Such a saddle point structure has no existence in our energy hypersurface. Therefore, this type of intramolecular proton transfer can most likely be neglected in favor of the simple rotational displacement of bicarbonate bound to zinc.

The TS **B6** corresponds to case IV in Scheme I. From the three possible interaction scenarios retained in Scheme I only cases II and III are present in the interconversion pathway calculated here.

Correlation Energy and Energy Hypersurface Shape. Correlation energy is calculated with MP2 procedure without geometry optimization (see Tables I, II, IV, and V). Figure 3 summarizes correlation effects on the SCF stationary points.

The energy of the reactants $[ZnOH^+ + CO_2]$ goes below **B2** TS energy. The gap shifts from −9.7 Kcal/mol to +16.3 Kcal/mol. This is the largest correlation effect on the gaps for this hypersurface found in the present calculations. The overall energy profile retains, however, the inverted shape found at the SCF level.

Correlation effects are also important for **B6**, but its energy remains well above reactants $[ZnOH^+ + CO_2]$ by 44 Kcal/mol. The energy gap between the TSs **B6** and **B2** decreases from 47 Kcal/mol at the SCF level to 28 Kcal/mol. This result is expected since **B6** is a bidentate complex and **B2** is monodentate and no intramolecular bond making/breaking process is going on in **B2**. In fact, the barrier between **B3** and **B6** decreases by 15 Kcal/mol due to correlation effects, but it remains large.

The energy barriers for the passage between **B1** and **B3** via **B2** increases by less than 4 Kcal/mol, while both reach the same energy level.

If the interconversion reaction were to be described as the passage from [$ZnOH^+ + CO_2$] via **B5–B4–B1** to **B2** as the product, then the energy difference between the extreme structures will control the kinetics.[16] As noted above, this gap is inverted at the SCF level. Moreover, one may expect geometry optimization at MP2 level will reinstall a double-well form for **B5–B4–B1** as it was found at the SCF level.

Correlation effects in absolute value are very large. Nevertheless, the relative changes are never larger than 27 Kcal/mol. At this point, it is important to realize that due to the cationic nature of the hypersurface, the inclusion of a coordination sphere or even of one water molecule might produce more significant changes in the energy gaps at the SCF level than correlation could produce. Moreover, differential correlation effects may be overcome by coordination sphere effects and solvation effects when ionic species are involved[16b] as it is shown later on.

IV. Bicarbonate/Water Exchange: $[ZnHCO_3H_2O]^+$ Hypersurface

The introduction of one water molecule in the model used to obtain the preceding hypersurface permits a more realistic description of the interconversion and exchange reactions, namely

$$ZnOH^+ + CO_2 + H_2O \rightarrow ZnHCO_3^+ + H_2O \rightarrow ZnH_2O^{2+} + HCO_3^-$$

By using the entries of Table I, the overall reaction presents an endothermicity of about 100 Kcal/mol smaller than without water. Moreover, the new hypersurface allows for studying the exchange of bicarbonate bound to zinc by a water molecule. One can proceed now, either by replacing zinc-bound bicarbonate with a water molecule (passive displacement solvation) or by adding a water molecule to react with zinc-bound bicarbonate (active solvation).

Active Solvation. Structures **B1**, **B2**, and **B3** describe three kinds of bicarbonate binding to zinc. At the level of CA active sites the maximal coordination number of zinc is 5. The protein contributes with three ligands. It can be reasonably assumed that, in order to let a water molecule access zinc, bicarbonate binding must be monodentate, such as in structure **B2**, for otherwise, there would be no accessible space for binding to zinc. Therefore, model hydration studies of **B1** and **B3** are not considered. Instead, solvation of the saddle point structure **B2** including one water molecule has been examined. In Figure 4 energetics and structural results are depicted.

The saddle points **C2c** and **C2t**, corresponding to carbonic acid moiety in cis and trans conformations, have been characterized. As there are no apparent differences among the isomers, the discussion is focused on the cis form.

The TV of **C2c** describes an intramolecular proton transfer between water and bicarbonate. The descents along the two directions of the TV lead to structures **C1c** and **C3c** depicted in Figure 4. Energetically, this TS is well below dissociation products [$ZnHCO_3^+ + H_2O$] and [$ZnOH^+ + cis\text{-}H_2CO_3$].

This TS **C2c** resembles the product (**C3c**) more than the reactant (**C1c**) and provides an illustration of Hammond's postulate. **C2c** describes a standard proton transfer assisted by a bond making/breaking process around zinc. Note that the existence of zinc transforms an otherwise bicenter proton transfer into a four-center process where two bonds are made while two others are broken.

The descent along the TV toward **C3c** corresponds to a virtual breaking of O4H2 and ZnO1 and simultaneous formation of ZnO4 and H2O1 bonds. The bicarbonate moiety does not significantly change along the path (see BOs in Table III). **C3c** has residual gradients (in mydnes Å/rad) over the angles O4ZnO1 (−0.01 at 90°) and ZnO1C (0.08 at 150°). At this point the structure is geometry optimized by keeping these angles constrained and the full Hessian is determined.

C1c is obtained by virtually breaking H2O1 and ZnO4 bonds and by simultaneously making ZnO1 and O4H2 bonds. The geometry and force constants have been determined in a similar manner to **C3c**; residual gradients are −0.12 and +0.04 for the angles O4ZnO1 and ZnO1C, respectively. **C1c** describes a zinc-bound bicarbonate solvated by water; bicarbonate ZnO1 bond is about the same as in structure **B2**, while water is 1.95 Å away. The effect of water is reflected in lowering the **BO** of the bicarbonate ZnO1 bond compared to **B2**, but otherwise it does not change significantly the force constant system of zinc-bound bicarbonate.

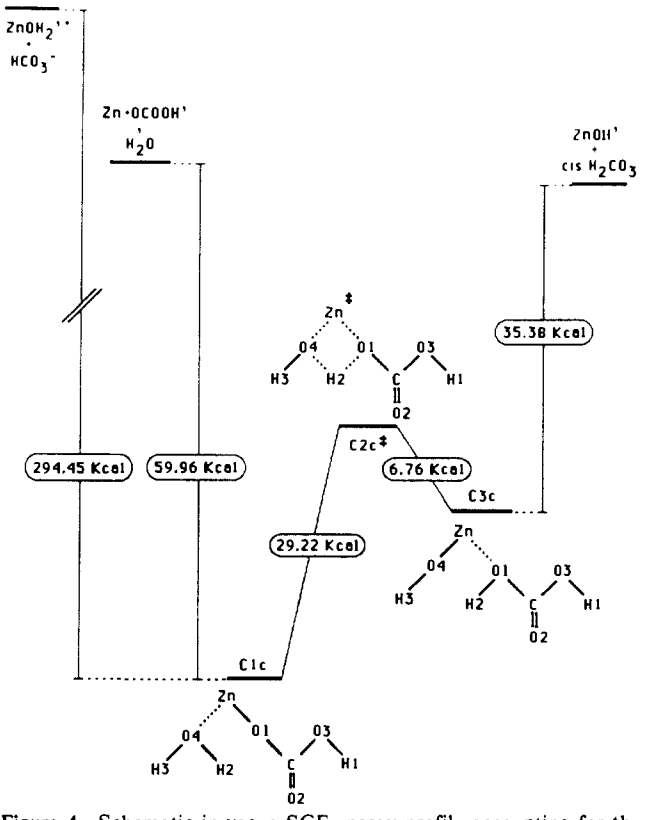

Figure 4. Schematic in vacuo SCF energy profile accounting for the $[ZnHCO_3H_2O]^+$ hypersurface. Pathway C corresponds to an active solvation of zinc-bound monodentate bicarbonate and describes a proton transfer between water and bicarbonate to produce carbonic acid. c and t stand for cis and trans. All the structures are planar. O3ZnO1C is 180°. For **C1** and **C3**, ZnO1C and O4ZnO1 are equal to 150° and 90°, respectively. SCF energies (au) and gradient lengths (mdyn) are −2116.301877, 1.85×10^{-4} for **C1c**; −2116.255311, 8.09×10^{-5} for **C2c**; −2116.266078, 4.52×10^{-4} for **C3c**; −2116.301543, 1.40×10^{-4} for **C1t**; −2116.255963, 3.91×10^{-5} for **C2t**; −2116.267008, 1.03×10^{-5} for **C3t**. The unique negative eigenvalues of **C2c** and **-t** are −2.33 and −2.26 mdyn/Å.

Passive Displacement Solvation. A solvation process, starting from [$ZnOH_2^{2+} + HCO_3^-$] and ending with [$ZnHCO_3^+ + H_2O$] is energetically favored in vacuo by 234 Kcal/mol as shown in Figure 4.

The displacement of bicarbonate by water in vacuo is an extremely large exothermic process. This is the result of separating the diionic species $ZnOH_2^{2+}$ and HCO_3^-. At the active site of the enzyme these partners are at finite intermolecular distances and surrounded by polarizable matter. Therefore, one would expect important surrounding medium effects.[40] To illustrate the effect of finite intermolecular distance, bicarbonate is placed near the water molecule bound to zinc (the distance O3O1 is equal to 2.3 Å). The energy gap becomes 35 Kcal/mol which, inci-

dentally, can be made smaller by reaction field effects.

An interesting result follows from this hypersurface. If a water molecule may enter the coordination shell while bicarbonate is bound to zinc the reactive channel for carbonic acid formation might be opened. As there is no firm experimental support for such pathway, one would prefer a displacement solvation process to take place at the active site.

V. Coordination Sphere Effects

A first step toward including essential constituents of the protein is via the inclusion of an ammonia coordination shell. In view of the ionic nature of the reactants one would expect large effects on the energy profiles.

Hydroxide Basicity and Nucleophilicity. The change of water acidity by zinc binding is commonly used to justify the zinc hydroxide mechanism. Variations in hydroxide proton affinity (PA) reflect this property and can be calculated by using entries in Table I. At an RHF level the PA of hydroxide is reduced by Zn^{2+} from 438 to 114 Kcal/mol; at the SCF–MP2 level the reduction is from 445 down to 107 Kcal/mol. The RHF figure is in reasonable agreement with the experimental value of hydroxide PA in vacuo ($\Delta H°_{298}$ ca. 390 Kcal/mol).[41] These results basically confirm former ab initio conclusions.[7-9]

The inclusion of the coordination shell formed by three ammonia molecules brings the PA of zinc-bound hydroxide up to 194 Kcal/mol (cf. Table I). The coordination shell increases the basicity strength of the bare zinc-bound hydroxide. Nevertheless, viewed from the in vacuo hydroxide standpoint, (ammonia) zinc-bound hydroxide has a lower basicity.

The coordination shell attenuates the zinc effect on the hydroxide nucleophilicity, but, in order to form bicarbonate, *it is still necessary to activate the carbonyl group.*

Note that charge transfer from hydroxide to zinc decreases from 0.50 to 0.13 by the effect of adding the coordination shell. Thus, the ligands modulate the zinc effect on the nucleophilic power of hydroxide PAs.

Thus, in vacuo the acidity of water is increased by its binding to zinc. In solution the pK_a of zinc-bound water decreases when compared to free water. Thus, it can be suggested that the in vacuo effect detected by the present calculations is reflected in the condensed phase behavior and a fortiori in the enzyme active site.

Bicarbonate Water Exchange. The TS **C2c** with the ammonia coordination shell has been estimated. The energy difference between $[ZnHCO_3^+ + H_2O]$ and $[ZnOH^+ + cis\text{-}H_2CO_3]$ favors now the former by 27 Kcal/mol. While **C2c** with model ligand shell moves 20 Kcal/mol below $[ZnHCO_3^+ + H_2O]$. The overall energy profile retains an inverted shape.

The energy difference between $[ZnOH_2^{2+} + HCO_3^-]$ and $[ZnHCO_3^+ + H_2O]$ decreases from 234 (without ligands) to 184 Kcal/mol (cf. Table I). The trend introduced by ligation is to facilitate bicarbonate displacement by water. The energy gap in vacuo is still large, but solvent effects might especially stabilize the ionic species $[Zn(NH_3)_3OH_2^{2+} + HCO_3^-]$. The displacement of water by bicarbonate and vice versa from zinc coordination shell in condensed phase will have similar energies.

$[Zn(NH_3)_3HCO_3]^+$ Hypersurface and Interconversion. As the coordination shell changes the energetics of zinc-bound molecules, it is important to know to which extent such changes may affect the nature of the stationary points described in section III.

A key feature of the bare zinc reactive hypersurface $[ZnOHCO_2]^+$ is its inverted shape. The transition structure **B2** which has the highest energy along this pathway is studied with the ammonia coordination shell in a tetrahedral (**T**) arrangement. A stationary point **B2T** on the $[Zn(NH_3)_3HCO_3]^+$ energy hypersurface has been characterized. Results are presented in Table VI and Figure 5.

The zinc bicarbonate moiety in **B2T** has a structure similar to **B2**. The average gradient length of **B2T** is 9×10^{-4} mdynes, and the total force constant matrix has been numerically calculated. Diagonalization of the Hessian leads to a fourth-order saddle point. The eigenvector associated with the lowest energy eigenvalue (−0.072) has the same structure as the transition vector in **B2**

Table VI. Geometry (Å and deg), Force Constants (mdyn/Å), and Transition Vector for the Saddle Point **B2T**[a]

variable	geom	*K*	C1
ZnO1	1.825	3.03	0.02
ZnN	2.077	1.21	
CO1	1.276	9.50	0.00
CO2	1.218	11.98	−0.01
CO3	1.381	5.70	0.03
H1O3	0.951	8.47	−0.00
NHa	1.004	7.15	
NHe	1.006	7.08	
ZnO2	3.999		
ZnO3	3.785		
ZnO1Du	94.9	−0.06	0.99
O1CO2	127.7	3.05	0.06
O1CO3	112.1	3.20	−0.05
H1O3C	112.5	0.79	−0.01
O1ZnN	107.3	0.26	
ZnNHa	118.8	0.73	
ZnNHe	107.7	0.78	
ZnO1DuC	180.7	0.06	−0.00
O3CO1O2	180.0	0.56	0.00
H1O3CO1	180.1	0.17	−0.00
O1ZnNHa	178.8	0.01	
NZnO1N	±120.4	0.24	
HeNZnHa	±122.5	1.05	

[a] SCF energy (au) and gradient length (mdyn) are −2208.980 297 and 9.42×10^{-4}, respectively. The first negative eigenvalue is −0.072 mdyn/Å.

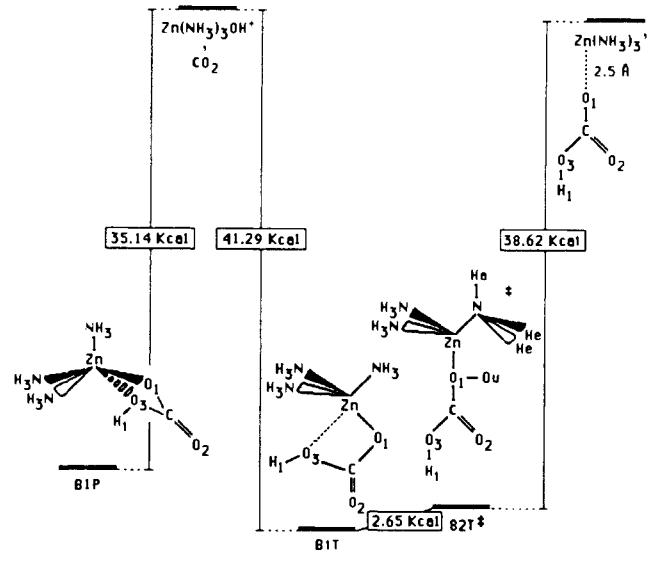

Figure 5. Schematic in vacuo SCF energy profile describing the ammonia coordination shell effects on zinc bicarbonate binding, according to tetrahedral (**T**) and pyramidal (**P**) arrangements. **B2T** is a saddle point over the full internal coordinate space; its first transition vector is only directed by the angle ZnO1Du as without ligation in **B2**. Note that the energy weel for **B2T** is four times deeper than it is without ligation (see Figure 1).

where ZnO1Du dominates the TV. The three other vectors having negative eigenvalues (−0.012, −0.007, and −0.004) describe dihedral displacements O1ZnNHa involving axial hydrogen atoms Ha (cf. Figure 5). Ten steps of energy minimization produce an average gradient of 3×10^{-4} mydnes, but the energy decreases by less than 0.009 Kcal/mol. The geometry does not change significantly, nonetheless, two of the negative eigenvalues disappear. The lowest eigenvalue (−0.087) has an eigenvector still dominated by the ZnO1Du variable (amplitude 0.94) and small coupling terms with the displacement of the hydrogen axial dihedrals whose amplitudes in the eigenvector amount to 0.18 in average.

The stationary points **B2T** and **B2** have basically the same nature, and both describe a rotation of bicarbonate around an axis drawn through the carbon atom and perpendicular to the carbonate plane. The geometry of HCO_3^- in **B2T** is planar now, and the

Table VII. Effective Charges for the Zinc Hydroxide and Carbon Dioxide Moieties in the Stationary Structures Described in This Study

	Zn	OH	CO_2
A1	1.56	−0.54	−0.02
B1	1.72	−0.38	−0.34
B2[‡]	1.71	−0.24	−0.47
B3	1.69	−0.15	−0.54
B4[‡]	1.73	−0.55	−0.18
B5	1.61	−0.63	0.03
B1T	1.67	−0.34	−0.54
B1P	1.68	−0.39	−0.49
B2T[‡]	1.70	−0.30	−0.61
B3T	1.68	−0.28	−0.62
B3P	1.66	−0.23	−0.63
HCO_3^-		−0.39	−0.61

zinc ion is also found in the carbonate plane.

Incidentally, the antisymmetric displacement of zinc and hydrogen atoms is described by the eigenvector having the smallest positive eigenvalue (0.049). The following eigenvalue (0.083) has an eigenvector where the largest amplitude is controlled by the ammonia umbrella angle O1ZnN. The dihedrals (NZnO1N) modulating the relative location of ammonia groups inside the coordination shell dominate the following eigenvector (0.104). The symmetric displacement out of the carbonate plane for Zn and bicarbonate proton has an eigenvalue of 0.165.

The structure **B2T** corresponds to a symmetrical tetrahedron, and the BOs of the four ligands are about the same (0.13). The force constant of ZnO1 is, however, larger than those for ZnN bonds, 3 and 1.2, respectively. The BO of ZnO1 is three times weaker than without ligands, and the force constant decreases significantly from 4.5 to 3. As a result, the bicarbonate moiety is less perturbed by zinc binding.

The force constants of the bicarbonate moiety in **B2T** are closer to free bicarbonate rather than to **B2** force constants. For instance, CO3 force constants in **B2**, **B2T**, and HCO_3^- are 7.1, 5.7 and 4.3, respectively. Furthermore, the effective charges in free bicarbonate for moieties OH and CO_2 (−0.39 and −0.61) are changed by bare zinc atom interaction into −0.24 and −0.47 in **B2** and restored by the ammonia ligands effect in **B2T** (cf. Table VII).

It is interesting to note than zinc ion changes its effective charge in a narrow band (1.56–1.73) for all models calculated here with and without ligands. The bonds made by zinc appear to be fairly ionic.

At this point, one should emphasize that the saddle point character of **B2** is conserved in presence of the ligands. The energy of **B2T** is below the one for reactants by about 38 Kcal/mol which is four times larger than without ligands. It remains to be shown where in the energy scale structures similar to **B1** and **B3** are located. In this paper we restrain the search to a descent along the directions of the TV without full geometric optimizations.[42]

The energy hypersurface is explored starting from the TS **B2T** by scanning the angle ZnO1Du responsible for the saddle point character in both directions. The total energy steadily descends as a function of the rotation angle.

As one increases the angle ZnO1Du, the force system in bicarbonate moiety reacts more strongly than the ammonia coordination shell. Perusal of the forces in the HCO_3^- moiety shows that by relaxing them a geometry resembling the structure **B1** would be attained (cf. Table VIII). A partial optimization leads to a structure 2.6 Kcal/mol below **B2T** named **B1T** in Table VIII. Rotation in the opposite direction by 35° conducts to a complex which is 1.7 Kcal/mol below the stationary point **B2T**; a partially geometry-optimized structure **B3T** is obtained. Analysis of the geometry and residual forces show that **B1T** and **B3T** should converge toward their analogues without ligands. Energy differences should not be dramatically changed as residual forces are relatively similar for these structures (**B1T** and **B3T**).

B1T and **B3T** as they stand correspond to distorted tetrahedral configurations. However, in **B3** HCO_3^- makes two equivalent bonds with zinc, and one would expect that a fully geometry-optimized **B3T** to fulfill the geometrical requirement for a pentaliganded complex.

Two models for pentacoordination are described in the literature: squared basis pyramid (P) and trigonal bipyramid.[43] An analysis of the Brookhaven protein data bank made by us shows that there are only two kinds of coordination states for zinc-containing enzymes: a tetrahedron and square basis pyramid.[44] The geometries described so far are related to a tetrahedral configuration, and it would be interesting to know where, in the energy scale, the counterparts having squared basis pyramid disposition are found. Complexes **B1P** and **B3P** have been constructed, partially optimized, and described in Table VIII. They are located 3.5 and −0.2 Kcal/mol relative to **B2T**, respectively.

B3P structure corresponds to a pentacoordinate complex around zinc. The BOs between oxygens or nitrogens atoms and zinc are nearly equal to 0.1. The coordination sphere weakens the zinc–oxygen bond order. The structure of the zinc bidentate bicarbonate moiety is about the same with and without ammonia ligands.

The two zinc–oxygen bonds in **B1P** are significantly different. The hydroxide oxygen O3 bond to zinc is three times weaker than the carbonyl oxygen O1 zinc bond (cf. Table III). The corresponding interatomic distances and BOs are 2.3 Å, 0.05 and 1.93 Å, 0.15, respectively. O3 occupies the fifth coordination site and does not make a strong bond with the metal. Note that in the free ligand complex (**B1**) a similar situation is found. The structure and bond order pattern of the bicarbonate moiety in **B1P** and **B1** are roughly the same. The coordination shell damps the charge transfer from bicarbonate and mainly affects the carbon dioxide moiety as Table VII shows.

A comparison of structures **B2T** and **B1P**, which is equivalent to the passage from **B2** to **B1**, shows that the carbon–hydroxide oxygen bond is weakened in a similar fashion. As noted in the study of the interconversion process initiated on **B1**, the structure **B1P** may be a starting point for searching the transition structure analogous to **B4**. In view of the subtle balances in the bond-forming/-breaking process and the abrupt inverted nature of the hypersurface in this region, a structure analogous to **B5** can only be obtained by descending along the reaction vector of the transition structure analogous to **B4**.

At this point we must emphasize that there has been retention of the inverted energy profile for any reasonable arrangement of ligands. Thus, an extrapolation is granted by the existence of complexes **B2T**, **B1P**, and **B1T**. One may reasonably expect the reactive energy profile found in the absence of ligands will have the same structure when model ligands are added.

The coordination state of zinc in the above structures may be four or five. The complexes **B1P** and to a lesser extent **B1T** are pentacoordinate models built out of four strong bonds and one significantly weaker. This result is suggested by the study of hypersurfaces without ligands. On the other hand, **B3T** is converging toward a pentaliganded model with five equivalent bonds, whereas **B3P** already has such a structure.

The coordination sphere brings down the energy difference for bicarbonate release by 125 Kcal/mol. This represents a decrease of about 36% of the bare zinc barrier. Note that a shift of about 0.7 Å in ZnO1 distance in **B2T** produces a complex having about the same energy than the reactant (cf. Figure 5).

The coordination state of zinc according to the present calculations suggest a shuttling between two forms: tetracoordination

(39) Calculation and diagonalization of the Hessian in a new frame without dummy atom, where the dihedral made by ZnO1CO2 plays the same role as ZnO1Du and has one negative force constant (−0.10), and the eigenvector describes the same rotation motion as in the preceding case.

(40) (a) Tapia, O.; Johannin, G. *J. Chem. Phys.* **1981**, *75*, 3624. (b) Tapia, O. In *Molecular Interactions*; Ratajczak, H., Orville-Thomas, W. J., Eds.; Wiley: Chichester, England, 1982; Vol. 3, Chapter 2. (c) Angyan, J.; Allavena, M.; Picard, M.; Potier, A.; Tapia, O. *J. Chem. Phys.* **1982**, *77*, 4723.

(41) Bartmess, J. E.; Scott, J. A.; McIver, R. T., Jr. *J. Am. Chem. Soc.* **1979**, *101*, 6056.

(42) The calculations have taken about 60 days of CPU time using one processor of Alliants FX-40 and FX-80. Full geometry optimizations of all other stationary states obtained for the bare zinc hypersurface $[ZnOHCO_2]^+$ with the ammonia coordination shell is beyond present computing capabilities at Uppsala.

Table VIII. Energies, Relative Energies, Gradients, and Internal Coordinates Derivatives Accounting for the Zinc Bicarbonate Moiety in the Structures Describing the $[Zn(NH_3)_3HCO_3]^+$ Hypersurface.

code	energy (au)	ΔE (Kcal/mol)	gradient (mdyne/Å)	internal coordinates derivatives (geometry)								
				ZnO1	CO1	CO2	CO3	O3H1	ZnO1Du	O1CO2	O1CO3	CO3H1
B2T[a]	−2208.980 297	0.00	9.4×10^{-4}	(1.82)	(1.28)	(1.22)	(1.38)	(0.95)	(94.9)	(127.7)	(112.1)	(112.5)
	−2208.980 540	−0.15	4.8×10^{-3}	−0.01	−0.01	0.01	−0.02	0.00	−0.01	−0.02	0.01	0.00
									(104.0)			
	−2208.981 129	−0.52	9.9×10^{-3}	−0.03	−0.03	0.03	−0.04	0.00	−0.01	−0.03	0.02	0.00
									(113.0)			
scan on ZnO1Du	−2208.982 024	−1.08	1.6×10^{-2}	−0.05	−0.04	0.04	−0.06	0.00	−0.02	−0.04	0.03	0.00
									(122.0)			
	−2208.983 044	−1.72	2.3×10^{-2}	−0.09	−0.06	0.05	−0.08	0.00	−0.01	−0.06	0.04	0.00
									(131.0)			
	−2208.983 628	−2.09	3.1×10^{-2}	−0.13	−0.09	0.05	−0.12	0.00	0.01	−0.08	0.04	0.00
									(140.0)			
	−2208.982 103	−1.13	4.9×10^{-2}	−0.21	−0.14	0.06	−0.15	0.00	0.10	−0.10	0.00	0.01
									(149.0)			
B1T	−2208.984 517	−2.65	1.8×10^{-2}	−0.06	−0.01	−0.03	−0.04	0.00	−0.01	−0.07	0.06	0.01
				(1.85)	(1.28)	(1.21)	(1.40)	(0.95)	(140.0)	(128.0)	(112.0)	(112.5)
B1P	−2208.974 714	3.50	2.4×10^{-2}	−0.08	−0.01	0.02	0.04	−0.00	−0.05	0.02	0.07	0.01
				(1.93)	(1.28)	(1.21)	(1.46)	(0.95)	(146.9)	(135.0)	(107.0)	(113.5)
B3T	−2208.983 005	−1.70	1.9×10^{-2}	−0.05	−0.01	−0.07	0.06	−0.01	0.03	0.07	−0.03	−0.00
				(1.82)	(1.28)	(1.22)	(1.38)	(0.95)	(60.0)	(127.7)	(112.1)	(112.5)
B3P	−2208.980 619	−0.20	2.5×10^{-2}	−0.01	0.04	0.02	−0.10	0.04	0.00	−0.08	0.03	0.03
				(2.09)	(1.27)	(1.28)	(1.32)	(0.96)	(91.0)	(116.0)	(122.2)	(118.0)

[a] T and P correspond to tetrahedral and pyramidal arrangements as shown in Figure 5. The geometry entries defining P are N–H = 1.006 Å, Zn–N = 2.11 Å; NZnN = 104.9° and ZnNH = 111.7°.

for bicarbonate binding (**B2T**) and a pentacoordination-like along the interconversion path. *To remain active, the zinc cation in our model never forms two simultaneous real bonds with the reactants.* This indicates an intrinsic property of zinc cation for this reaction.

VI. On the Catalytic Mechanism of Carbonic Anhydrases

In mammals, six isoenzymes have been isolated so far, three of them, CAI, -II, and -III, have been crystallized and their structures determined at high resolution.[29-31] In the literature, CAI and CAII are referred as high activity forms, while CAIII is a low activity one. Available kinetic data indicate that CAI and CAII have a common mechanistic pattern.[1a,45,46]

Zinc Hydroxide Catalytic Mechanism. A simplified model of the catalytic mechanism of HCAII is depicted in Scheme II;[1,3,4,29-31,45-64] it summarizes a wealth of experimental information thoroughly reviewed by Lindskog and Silverman.[1,3,4]

Scheme II

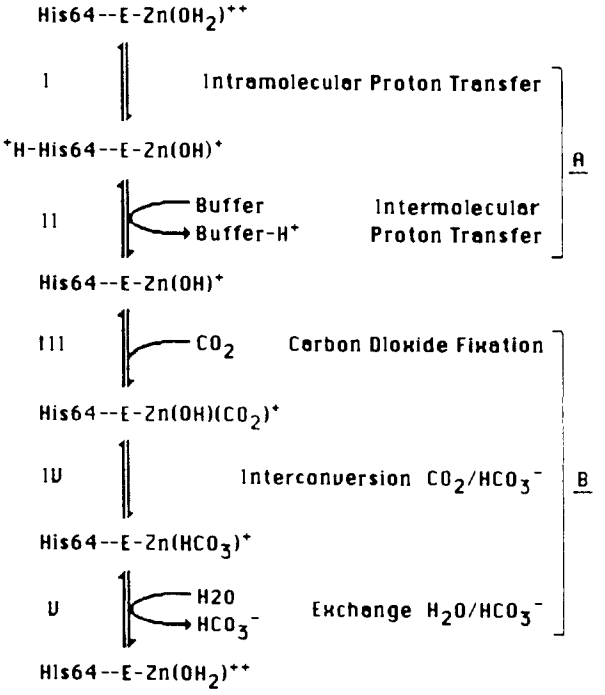

The mechanism covers two general processes: (i) Zn–water activation and (ii) an exchange between carbon dioxide and bicarbonate. They are designated as A and B in Scheme II.

Zn–water activation corresponds to a proton release to the medium. The generally accepted mechanism for this process in HCAII calls for an intramolecular proton transfer between zinc-bound water and His-64 (step I) and an intermolecular proton transfer between His-64 and the buffer (step II).

His-64 is required for high CO_2 hydration activity and participates in a proton relay structure with Zn–water.[4,47] Some confusion has arisen concerning the role played by His-64 as a

(43) Cotton, F. A.; Wilkinson, G. *Advanced Inorganic Chemistry*; Interscience: New York, 1982.
(44) Argos, P.; Garavito, R. M.; Eventoff, W.; Rossman, M. G.; Brändén, C.-I. *J. Mol. Biol.* **1978**, *126*, 141.
(45) Khalifah, R. G. *J. Biol. Chem.* **1971**, *246*, 2561.
(46) Simonsson, I.; Jonsson, B. H.; Lindskog, S. *Eur. J. Biochem.* **1982**, *129*, 165.
(47) Tu, C.; Wynns, G. C.; Silvermann, D. N. *J. Biol. Chem.* **1981**, *256*, 9466.
(48) Silverman, D. N.; Tu, C. K. **1975**, *97*, 2261.
(49) Jonsson, B. H.; Steiner, H.; Lindskog, S. *FEBS Lett.* **1976**, *64*, 310.
(50) Venkatasubban, K. S.; Silvermann, D. N. *Biochemistry* **1980**, *19*, 4984.
(51) Steiner, F.; Jönsson, B. H.; Lindskog, S. *Eur. J. Biochem.* **1975**, *59*, 253.
(52) Pocker, Y.; Bjorkquist, D. W. *Biochemistry* **1977**, *16*, 5698.
(53) Simonsson, I.; Jonsson, I.; Lindskog, S. A. *Eur. J. Biochem.* **1979**, *93*, 409.
(54) Bertini, I.; Borghi, E.; Luchinat, C. *J. Am. Chem. Soc.* **1979**, *79*, 7070.
(55) Silverman, D. N.; Tu, C. K.; Lindskog, S. A.; Wynns, G. C. *J. Am. Chem. Soc.* **1979**, *101*, 6734.
(56) Paneth, P.; O'Leary, M. H. *Biochemistry* **1985**, *24*, 5143.
(57) Paneth, P.; O'Leary, M. H. *Biochemistry* **1987**, *26*, 1728.
(58) Khalifah, R. G. *Proc. Natl. Acad. Sci. U.S.A.* **1973**, *70*, 1986.
(59) Lindskog, S.; Coleman, J. E. *Proc. Natl. Acad. Sci. U.S.A.* **1973**, *70*, 2505.
(60) Pocker, D. A.; Deits, T. L. *J. Am. Chem. Soc.* **1982**, *104*, 2424.
(61) Tibell, L.; Forsman, C.; Simonsson, I.; Lindskog, S. *Biochim. Biophys. Acta* **1984**, *789*, 302.
(62) Eriksson, E. A.; Kylsten, P. M.; Jones, T. A.; Liljas, A. *Proteins* **1988**, *4*, 283.
(63) Forsman, C.; Behravan, G.; Jonsson, B.-H.; Liang, Z.-w.; Lindskog, S.; Ren, X.; Sandström, J.; Wallgren, K. *FEBS Lett.* **1988**, *229*, 360.
(64) Williams, T. J.; Henkens, R. W. *Biochemistry* **1985**, *24*, 2459.

proton transfer group.[62] Its replacement with other residues (Lys, Ala, Glu, and Gln), by site-directed mutagenesis, caused only a small reduction in the carbon dioxide hydration activity according to the results reported by Forsman et al.[63] In fact, these experiments were done with 1,2-dimethylimidazole/*m*-cresol purple as a buffer indicator system thereby providing with a substitute for the replaced His-64. Histidine 64 is necessary for high carbon dioxide hydration activity of HCAII as it has recently documented with new experiments made by Lindskog and Silverman groups.[65] A buffer dependence of the turnover rates (step II) has been documented.[1,48-50] At low buffer concentration an intermolecular proton transfer involving the buffer is rate-limiting step;[49] at high buffer concentration the rate-limiting step is an intramolecular proton transfer.[51,52] The intermolecular proton transfer occurs in a step separated from the CO_2/HCO_3^- exchange, and this latter is not buffer dependent.[53]

The exchange process corresponds to steps III, IV, and V in Scheme II. Carbon dioxide fixation would proceed without making a tight bond to the metal as suggested by Bertini et al.[2,54] and Lindskog.[1b] In fact, binding of a neutral ligand such as CO_2 must be weaker than an ionic ligand, such as HCO_3^-.

The key mechanistic step is the interconversion CO_2/HCO_3^- (step IV in Scheme II), and there is no rate-limiting proton transfer during this interconversion.[51,53,55-57]

The interconversion step is assumed to occur by direct nucleophilic attack of zinc-bound hydroxide on carbon dioxide and not by a general base mechanism wherein zinc-bound hydroxide abstracts a proton from an adjacent water, whereas the incipient hydroxide reacts with CO_2.[4,52]

The dissociation rate of HCO_3^- from zinc coordination sphere is a fast process.[2,54]

Theoretical Characterization of the Interconversion Pathway. An energy profile for the interconversion between carbon dioxide and bicarbonate summarizing the theoretical results discussed in the preceding sections is depicted in Figure 6.

The essential feature is the inverted nature of the energy profile. Discrete solvation and coordination shell effects enhance this trend found for the bare zinc energy profile. In fact, the saddle point **B2** which has the highest energy in the well (10 Kcal/mol below reactants) is pushed down by about 40 Kcal/mol with respect to ammonia-liganded reactants. Correlation effects would at most decrease this difference by 26 Kcal/mol on the relative position of **B2**. For this reason **B2** is safely assumed to be located below reactants.

The nature of the saddle point **B2** is not changed by the inclusion of coordination shell. The displacement along the transition vector brings the system downwards in energy toward a structure similar to **B1**. The study of **B1P** indicates that the interconversion path will lie at the bottom of the well and will proceed in a way similar to the bare zinc model.

The energy position of **B6** is well above **B2** and reactants. The calculation including the coordination shell shows at the SCF level that the energy gap between the two saddle points is about 50 Kcal/mol. Correlation effects would decrease this entry by about 20 Kcal/mol thereby leaving this point well above not only **B2** but also the reactants. The profile clearly shows that an intramolecular proton transfer is unlikely to occur since it has an extremely large activation energy. This is in agreement with the fact that there is no rate-limiting proton transfer during the interconversion process.[51,53,55]

The relative energy level of products has been chosen by using our calculations of a complex where bicarbonate is at 2.5 Å from zinc. As shown in Figure 5 reactants and products may have nearly zero energy gap. The important point is that the enzyme may modulate this energy gap since the products involved have a diionic structure. This type of solvent effects is well documented.[40]

The interconversion process in Scheme II is well represented by the passage **R-B5-B4-B1-B2-P** depicted in Figure 6.

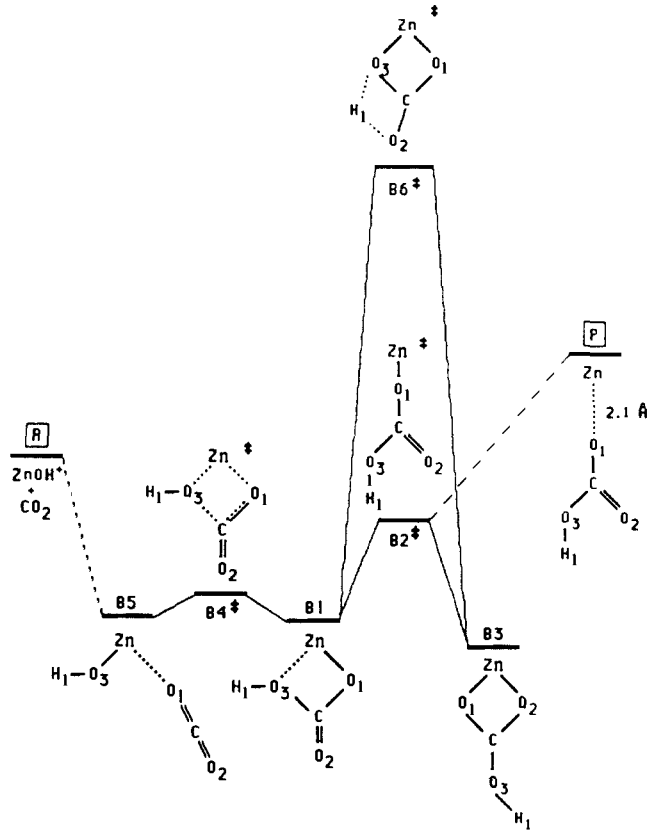

Figure 6. Schematic energy profile describing an interconversion pathway between reactants (R) represented by $ZnOH^+$ and CO2 and products (P) represented by the intermolecular complex $Zn^+\cdots HCO3^-$. This profile summarizes the results obtained in the present ab initio study.

The saddle point **B2** represents both bicarbonate fixation for the dehydration reaction and bicarbonate displacement by water for the opposite reaction; this is the hypothesis retained here. A simultaneous binding of bicarbonatte and water to zinc is formally excluded, for, if a water molecule binds **B2**, the channel leading for carbonic acid might be opened. Experimental studies clearly indicate that H_2CO_3 is unlikely to be the product of the catalytic reaction.[58,59,1b]

The theoretical results commented so far indicate that zinc must have only four real ligands to permit a catalytic pathway as the one shown in Figure 6. Complexes like **B3** or any stable minima showing pentacoordination will more than likely behave as inhibitors because they will freeze the fifth coordination site. This statement is reinforced by experimental works[60-62] such as the crystallographic studies of inhibitor-binding sites in HCAII.[62] This argument gains more force if one looks at the model enzyme system designed by Tabushi and Kuroda.[15b] These authors have found that bicarbonate formation inhibit the model enzyme activity.[15a,b] Furthermore, the choice of **B2** warrants microreversibility[66] which is an essential point for any mechanistic proposal.

The saddle point **B4** corresponds to the transition state for interconversion. This transition structure shows a complex set of atomic displacements requiring the zinc cation to have a disponsibility for pentacoordination. If the fifth position is occupied by any ligand, such a chemical rearrangement cannot take place.

Interestingly, the saddle point structure **B4** accounting for the interconversion step provides a rationale for the proposed transfer of an OH^- moiety from bicarbonate to zinc as discussed by Lindskog et al.[1]

The nature of complex **B5** clearly suggests that carbon dioxide does not form a strong chemical bond with zinc. The result given is not contradicted by the fact that there is a fast exchange of carbon dioxide with the active site.[1] On the other hand, as the

(65) Tu, C.; Silverman, D. N.; Forsman, C.; Jonsson, B.-H.; Lindskog, S. *Biochemistry* **1989**, *28*, 7913.

(66) Albery, W. J.; Knowles, J. R. *Biochemistry* **1975**, *15*, 5631.

structure **B4** suggests, there would be no direct nucleophilic attack of zinc-bound hydroxide onto carbon dioxide unless the carbonyl group is activated by zinc. Thus, the accepted description of a direct nucleophilic attack is not warranted by the present study.

For an inverted profile such as the one of Figure 6, the kinetics of interconversion **R** → **P** is controlled by the energy difference between them. A warning concerning the inverted energy profile is necessary at this point. While the inner complexes represented by **B5–B4–B1–B2** are a result of direct electronic interactions with the metal and their relative energy differences would probably be kept in an enzyme environment, the relative energies of **R** and **P** are bound to be modified. Our results are obtained for a system in vacuo, and the extrapolations made here must be considered as a hypothesis that has to be validated with further studies.

As pointed out by one of the referees, one of the main conclusions of this paper is that carbon dioxide must first be activated by the zinc before the nucleophilic attack by the hydroxide. This conclusion is true in the gas phase, but it must be qualified when extrapolations are made to describe the reaction in solution or protein environments. In solution, carbon dioxide is solvated, and the problem of catalysis by a solvated zinc ion would demand a more sophisticated model than the one used here. At the active site of the enzyme the situation is less complex. There is no place for a solvated carbon dioxide to enter the coordination shell of a zinc hydroxide complex. Any barrier concerning solvation–desolvation of carbon dioxide acts at a stage different from the interconversion process. Thus, once such a barrier is overcome, the process is basically (not fully) described by the present calculations. The interconversion half-reaction in the CAs mechanism described so far is basically due to the zinc cation properties, and if it follows the inverted energy profile this step cannot be rate-limiting.

Active Site Constraints. In order to check the plausibility of the theoretical mechanism proposed above, manual docking studies have been made. If the structures calculated in vacuo can be docked without steric hindrances from the active site residues, the intramolecular forces of the quantum motifs are likely to dominate against the more weak intermolecular one. Such a procedure gives qualitative hints only.

Considering that **B2** is (i) a saddle point due to zinc independent of a coordination shell, (ii) an opening gate toward interconversion, and (iii) the only point accounting for water/bicarbonate exchange, this structure has been docked at the active site of HCAI, HCAII, and BCAIII. The structure obtained represents a model for direct bicarbonate binding. This model complies with requirements based on experimental information.[2,54,1b]

In Figure 7a the structure **B2** docked at HCAII active site is depicted. The enzyme structure has not been modified but, of course, water bound to zinc has been removed. Such "rigidity" of the protein structure is granted by results from the crystallographic work of Eriksson et al.[62] The structure **B2** has only one degree of freedom which conserves the tetrahedral structure around zinc, while allowing for a rotation of bicarbonate moiety along the CO1 axis. Oxygen O2 has been located equidistantly between OG1 of Thr-199 (2.3 Å) and the deep water (DW) molecule (2.2 Å). As a result, O2 is 2.0 Å away from the Thr-199 NH group. The hydroxyl moiety is directed toward the entrance of the active site. The oxygen bound to zinc (O1) is 2.8 and 2.7 Å away from Thr-199 hydroxyl oxygen (OG1) and deep water, respectively.

Bicarbonate binding in HCAII (cf. Figure 7a) would mainly be due to hydrogen bonding with the deep water and the Thr-199. It is important to note that the hydroxyl group of Thr-199 is now in front of two highly charged bicarbonate oxygens (O1 and O2); consequently, one would expect its proton to be redirected from OE1 Glu-106 toward these new H-bond acceptors. With this rearrangement, Thr-199 is made to play an essential role in catalysis. This binding does not modify the structure of **B2** and it can be thought of as opening the reactive gate which leads to bicarbonate dehydration path, namely, **B1–B3–B4**.

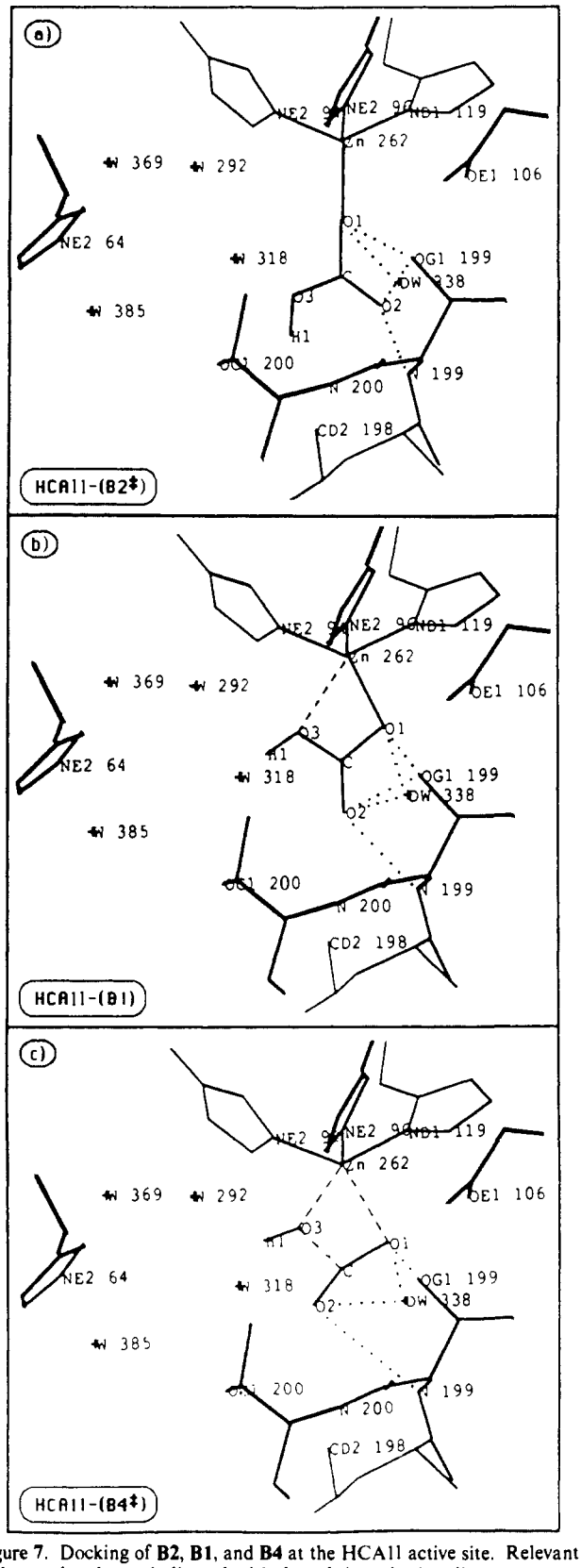

Figure 7. Docking of **B2**, **B1**, and **B4** at the HCAII active site. Relevant hydrogen bonds are indicated with dotted lines; broken lines represent bonds in the process of being broken or formed. The deep water is indicated as DW and water molecules as W; amino acids drawn in this picture are histidines-64, -94, -96 and -119, threonines-199 and -200, leucine-198, and glutamic acid-106.

A rotation following the direction of **B2**'s transition vector can be performed without steric hindrance. In Figure 7b a structure analogous to **B1** is depicted.

In **B1** the zinc-bound oxygen O1 approaches to OG1 (2.2 Å), remaining at 2.8 Å from the deep water. Oxygen O2 moves within

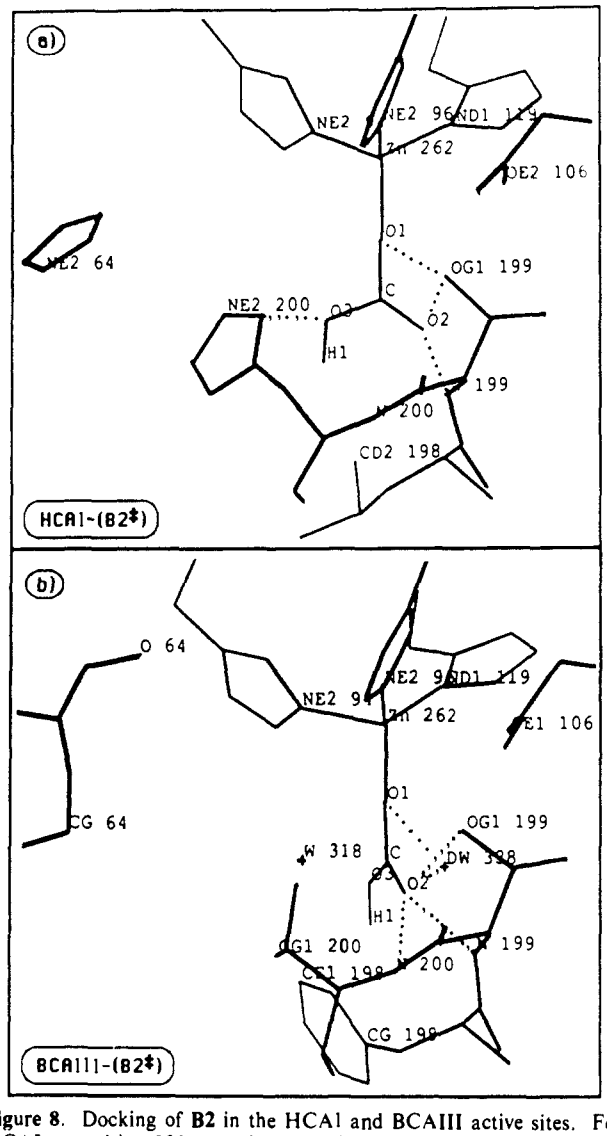

Figure 8. Docking of **B2** in the HCAI and BCAIII active sites. For HCAI at position 200 there is a histidine which may H-bond the hydroxyl moiety of our bicarbonate productive binding structure; histidine-64 is also drawn to help visualize the active site entrance direction. For BCAIII the residue 198 is now a phenylalanine. The H-bond pattern also involves the N–H groups of residues 199 and 200. Note that Lys-64 replaces histidine.

H-bond distance to OG1 (2.8 Å), at 2.5 Å distance from the deep water, and 2.6 Å from NH of Thr-199. In the present model, a displacement from **B2** to **B1** does not change the number of H-bonds with the enzyme.

Replacing the structure **B1** by **B4** in the active site one gets Figure 7c. O1 is now 2.3 Å from OG1-199 and 2.4 Å from the deep water. The atom O2 is now located at more than 3 Å from the residues lining the active site.

Figure 7a–c show that the theoretical mechanistic pathway can be plausibly accommodated at the active site level. Here, Thr-199 plays a central role. Its absence would open the way for a bidentate bicarbonate binding channel which, according to our views, would inhibit the present catalytic mechanism.

Hints concerning the different activities due to fine-tuning for CAI and CAIII can be obtained by docking **B2** in their active sites. Bicarbonate productive binding to these active sites are displayed in Figure 8 (parts a and b, respectively). HCAI presents a new interaction with bicarbonate via NE2 of His-200 (2.7 Å from O3) which would explain the difference in stabilization of the enzyme–HCO_3 complex between isoenzymes I and II.[2,44,64] BCAIII presents an interesting H-bond pattern. Atom O2 is engaged in four H-bond contacts: deep water (2 Å), OG1 Thr-199 (2.7 Å), NH-199 (2.2 Å), and NH from Thr-200 (3.1 Å). The hydroxyl group interacts with the side chain of Phe-198. A slight rotation of this ring puts the hydrogen into π-hydrogen bond disposition. Two new H-bond contacts are present here which would contribute to explaining its low catalytic efficiency by increasing the barriers along the catalytic pathway discussed above.

VII. Discussion

Transition structures corresponding to interconversion and productive binding of bicarbonate have been characterized, and a mechanistic scheme has been presented. Eriksson et al. have proposed a detailed mechanistic scheme[62] which is consistent with the one suggested by Kannan et al.[67] The former differs from ours in the binding sites used by the reactants during catalysis. Three binding sites A, B, and C are distinguished by them.[62] Site A on the zinc cation is found between the B and C sites and assigns a tetrahedral geometry (including of course histidine ligands) to zinc. The inhibitor thiocyanate (SCN^-) binds to site B at van der Waals' distance of OG1 atom of Thr-199 with displacement of the deep water. Site C lies at the opposite side opening toward the entrance of the active site cavity. These authors suggest that a bicarbonate ion can be placed with its negative charge at site B and its protonated oxygen at site C. In our proposal, bicarbonate binds at site A, site B is not fully accessible due to the presence of the deep water, and, as bicarbonate rotates to take the interconversion pathway, it does it by using site A to position the hydroxyl group. Thus, the spatial arrangement for the structure equivalent to our complex **B1** (structure D in Figure 9 of ref 62) is just the opposite to the one selected by us. This enforces a difference with respect to carbon dioxide binding also (cf. structure B of Figure 9 in ref 62 and our **B5** and Figure 7c where **B4** is docked showing the position of carbon dioxide). Carbon dioxide is a weak ligand.[2] In the structure proposed in Figure 7, Glu-106 and hydroxyl at site C produce enforced electrostatic induction forces which might help docking this apolar molecule; the quadrupolar field made by Glu/Zn/OH may interact with the quadrupolar moment of carbon dioxide also. Since our calculations show that the nucleophilic power of $ZnOH^+$ is annihilated along a direct docking line, which is implied in Figure B of ref 62, the natural path to take would be to follow the attractive versant of the energy hypersurface. This latter enforces binding at nearby site A overlapping somewhat with site B, the hydroxyl ion moving away from zinc simultaneously. Of course, in our situation, the carbon dioxide moiety is facing Thr-199, and we claim a new pattern of hydrogen bonding: this time OG1 hydrogen is redirected toward this highly charged moiety which allows us to assign Thr-199 an essential role in catalysis by preventing formation of the bidentate bicarbonate binding. This latter will take binding sites B and C and would deactivate the enzyme.[60] A site-directed mutagenesis replacing this residue by a nonpolar group would alter the catalytic properties of this active site in a profound way. This prediction provides with an experimental test which may decide between these two different mechanistic proposals.

An internal proton transfer within the bicarbonate molecule has been proposed by Liang and Lipscomb.[9,10,68] Experimentally, it is known that there is no rate-limiting proton transfer during interconversion. This does not mean of course that a proton transfer with low barrier might not be there as suggested by these authors. The mechanism proposed by us does not require such intramolecular proton transfer; it solves the problem in a different way via molecular rotations.

The structures reported by A. Pullman and co-workers[6–8] compare fairly well with some of the minima calculated here. As no characterization via diagonalization of the Hessians was performed by these authors, a comparison is difficult. Nonetheless, their results and ours are fairly complementary. As the basis set used in our calculations are near Hartree–Fock limit, a good deal of credibility can be assigned to the structures, force constants, and energies reported in the present work.

In a recent paper by Merz et al.,[69] AM1 semiempirical MO

(67) Kannan, K. K.; Petef, M.; Fridborg, K.; Cid-Dresdner, H.; Lövgren, S. *FEBS Lett.* **1977**, *73*, 115.
(68) Liang, J. Y.; Lipscomb, W. N. *Int. J. Quantum Chem.* **1989**, *36*, 299.

calculations are reported; this paper addresses several points treated here. The reaction profile for the hydration of carbon dioxide and active solvation of bicarbonate bound to zinc has striking similarities to ours. The geometry of their structure **28** resembles our saddle point **B4**. For active solvation, their structure **35** looks also similar to our **C2t**. The activation barriers obtained with AM1 are, however, rather large.

When the present structural data are compared to those obtained with AM1, it appears that this particular empirical method is fairly successful in rendering transition structures for the interconversion process. This is good news since computing costs are unbearable when ab initio calculations are carried out at the level of basis set enterprised here. Unfortunately, the energetics of AM1 for the reaction profiles is profoundly at variance with our calculations and those by Pullman's group. The difference concerns both the shape of the energy profiles and activation barriers. The actual shape of the hypersurface for this type of reaction is essential for describing the molecular mechanism.

The mechanistic role of zinc in carbonic anhydrases appears to be rather complex. Hydroxide bound to zinc becomes a poor nucleophile. The carbonyl function must be activated before a nucleophilic attack (hydroxylation) may take place. The present theoretical results provide a fairly different picture of nucleophilicity when compared to the standard model.[1,4,6-8,9b] For the molecular events occurring at the level of the zinc coordination shell in the enzyme during interconversion, we suggest, as a hypothesis, that the corresponding energy profile has an inverted shape where the energy difference between **R** and **P** (cf. Figure 6) is controlled by surrounding medium effects.[70-72]

Acknowledgment. Olivier Jacob gratefully acknowledges financial support from Merrell Dow Research Institute. Orlando Tapia thanks the Swedish Research Council for financial assistance. We are grateful to Mons Ehrenberg from BMC, who also got into the inverted profile hypothesis from a completely different path, for invaluable discussions. We thank Profs. S. Lindskog, E. M. Evleth, and R. Bywater for reading the manuscript and for giving us helpful advice. We are also indebted for the constructive comments from the referees.

Registry No. CO_2, 124-38-9; $Zn(OH)^+$, 22569-48-8; $Zn(NH_3)_3OH^+$, 72147-20-7.

(69) Merz, K. M., Jr.; Hoffman, R.; Dewar, M. J. S. *J. Am. Chem. Soc.* **1989**, *111*, 5636.

(70) The energy difference between **R** and **P** may be modulated by enzyme and solvent effects[40,71,72] because the product, bicarbonate zinc ion, has an ion-pair nature, while the reactant is a neutral molecule interacting with an ion; consequently, the energy difference between reactant and product can be reduced and fine tuned by the enzyme system.[40,72] Now, for an inverted type of energy profile, the kinetics are determined by the energy difference between reactants and products, while differential kinetic efficiency among isozymes would be dependent upon the detailed path for interconversion at the bottom of the well. Experimental and theoretical work on inverted potential energy shape for gas-phase nucleophilic displacement reactions[17] and carbo-acid strength[16] have documented such behavior. Consequently, the rate-limiting step for the reaction must be found at the other stages of the mechanism depicted in Scheme 11.[1,3,4]

(71) Sheridan, R. P.; Allen, L. C. *J. Am. Chem. Soc.* **1981**, *103*, 1544.

(72) (a) Warshel, A.; Sussman, F. *Proc. Natl. Acad. Sci. U.S.A.* **1986**, *83*, 3806. (b) Warshel, A.; Weiss, R. *J. Am. Chem. Soc.* **1980**, *102*, 6218.

Electronic Structure of Icosahedral Cobalt-Sulfur Clusters

Gary G. Hoffman,† James K. Bashkin,‡ and Martin Karplus*

Contribution from the Department of Chemistry, Harvard University, Cambridge, Massachusetts 02138. *Received January 22, 1990*

Abstract: This paper uses the multiple scattering (MS)-Xα method to calculate the electronic structure of several clusters that contain an octahedral Co_8S_6 core. Two of the clusters are analogous to compounds that have been previously synthesized, and the results of these calculations are consistent with the experimentally observed spin states, absorption spectra, and structural similarity of these compounds. These clusters are of particular interest because they are related to the component structures of the mineral cobalt pentlandite. To obtain information that can be extended to cobalt pentlandite, the effects of oxidation state and added ligands to the core structure of the clusters are studied. An extended Hückel theory (EHT) study of similar clusters has been performed by Burdett and Miller. In addition to MS-Xα results, we present EHT calculations on clusters of lower symmetry than those studied by Burdett and Miller. The spectra from the two types of calculations correspond in general and the central conclusions of Burdett and Miller are supported by the MS-Xα results. However, because the MS-Xα calculations take account of the electron-electron interactions explicitly, they provide more rigorous information on the effects observed. Specifically, the cobalt-sulfur bonding orbitals are observed to form a separate lower energy band whose structure varies upon addition of ligands to the cluster, spin pairing is found not to be important in determining the ground-state configurations, and the tendency of the cluster to contract upon addition of ligands is found to be due to an overall redistribution of charge rather than to any specific orbitals.

1. Introduction

Metal sulfide minerals offer a wide variety of structures, some with "extraordinary physical properties"[1] that stem from the fact that they are extensively interconnected and are not decomposable into independent molecular building blocks. However, there exists a class of these compounds that is made up of extended lattices of recognizable metal sulfide clusters that are connected by bridging interactions. The most famous of these substances are probably the Chevrel phases of the molybdenum chalcogenides,[2] which have unusual conducting properties. Pentlandite is a

Table I. Average Bond Distances (Å)[a]

	$[Co_8S_6(SPh)_8]^{4-b}$		$[Co_8S_6(SPh)_8]^{5-b}$	pentlandite $(Co_9S_8)^c$
	anion 1	anion 2		
Co-Co	2.662	2.653	2.674	2.505
Co-S_b	2.230	2.226	2.236	2.227
Co-S_t	2.239	2.242	2.276	2.127

[a] The bond lengths for the salts are average values, with the individual bond lengths differing by as much as 0.02 Å from the mean. [b] Reference 5. [c] Reference 30.

† Present address: Department of Chemistry, Florida International University, Miami FL 33199.

‡ NIH postdoctoral fellow, 1984-1985. Present address: Monsanto Co., 800 N. Lindbergh Boulevard, St. Louis, MO 63167.

0002-7863/90/1512-8705$02.50/0